where

$$E = E_0 r_0/r$$

and

$$E_0 = \text{field at } r_0$$

If the phase velocity of the wave is $u$, all the accelerations can be referred back with the proper phase and amplitude as though they occurred at the inner boundary of the medium at $r_0$. Thus, the velocity $W_0$ of a vibrating electron in the wave which started at $r_0$ at the time $t_0$ is, when referred back to $r_0$ (using the relation given in (12) that $|\dot{r}| \propto r^{-1/2}$), given by

$$W_0 = \int_{r_0}^{R} \sqrt{\frac{r}{r_0}} \frac{eE_0}{mur} \cos\left(\phi_0 - \omega \frac{r - r_0}{u}\right) dr$$

$$= \frac{eE_0}{mu\sqrt{r_0}} \cdot \int_{r_0}^{R} \frac{\cos\left[\phi_0 + (\omega r_0/u) - (\omega r/u)\right]}{\sqrt{r}} dr \quad (1)$$

where

$$\phi_0 = \omega t_0$$

The integration can be performed in terms of Fresnel integrals to give

$$W_0 = \frac{eE_0}{m_0}\sqrt{\frac{2\pi}{ur_0\omega}}\sqrt{C^2 + S^2} \cdot \cos\left(\phi_0 + kr_0 - \arctan\frac{C}{S}\right) \quad (2)$$

$$k = \omega/u = \text{propagation constant}$$

$$C = C(kR) - C(kr_0) \quad (3)$$

$$S = S(kR) - S(kr_0) \quad (4)$$

and $C(x)$ and $S(x)$ are tabulated by *Jahnke and Emde* [1945]. The cosine term in (2) is time-dependent since

$$\phi_0 = \omega t_0$$

so that

$$|W_0| = \frac{eE_0}{m}\sqrt{\frac{2\pi}{ur_0\omega}}\sqrt{C^2 + S^2} \quad (5)$$

As $R \to \infty$, i.e., the integration is performed from the inner boundary out to infinity,

$$C \to 0.5 - C(kr_0)$$

$$S \to 0.5 - S(kr_0)$$

The ratio

$$W_0/w_0 = \sqrt{2\pi}\sqrt{kr_0}\sqrt{C^2 + S^2} = B(kr_0) \quad (6)$$

where $w_0$ is given in (9) in this paper. A plot of (6) as a function of $kr_0$ is given in Figure 2. If $r_0$ is the ion sheath radius, which is commonly of the order of a few Debye lengths, we have (assuming $r_0 = 4\lambda_D$)

$$kr_0 = 8\pi\lambda_D/\lambda = 4\omega\sqrt{K}/\omega_p\sqrt{\gamma} \quad (7)$$

Since $K$ is a function of $\omega_p/\omega$, and $X = 1 - (\omega_p^2/\omega^2)$, $B$ can also be plotted as a function of $X$ as in the upper scale of Figure 2.

## References


Bauer, S. J., and R. Bourdeau, Upper atmosphere temperatures derived from charged particle observations, *J. Atmospheric Sci., 19,* in press, 1962.

Bohm, D., and E. P. Gross, Theory of plasma oscillations, *Phys. Rev., 75,* 1851–1876, 1949.

Jackson, J. E., Rocket-borne instrumentation for ionosphere propagation experiments, *Naval Res. Lab. Rept. 3909,* 1957.

Jackson, J. E., and J. A. Kane, Breakdown and detuning of transmitting antennas in the ionosphere, *Naval Res. Lab. Rept. 5345,* 1959.

Jackson, J. E., and A. D. Pickar, Performance of a rocket-borne 7.75 Mc/s transmitting antenna in the ionosphere, *Naval Res. Lab. Rept. 4911,* 1957.

Jahnke, E., and F. Emde, *Tables of Functions,* p. 35, Dover Publications, New York, 1945.

Jastrow, R., and G. A. Pearse, Atmospheric drag on the satellite, *J. Geophys. Res., 62,* 413, 1957.

Kane, J. A., J. E. Jackson, and H. A. Whale, The simultaneous measurement of ionospheric electron densities by CW propagation and RF probe techniques, *NASA Tech. Note D-1098,* 1962.

Landau, L., On the vibrations of the electronic plasma, *J. Phys. USSR, 10*(1), 25–35, 1946.

Spitzer, Lyman, *Physics of Fully Ionized Gases,* p. 59, Interscience Publishers, New York, 1956.

Stratton, J. A., *Electromagnetic Theory,* McGraw-Hill Book Co., New York, 1941.

Whale, H. A., Ion sheath effects near antennas radiating within the ionosphere, *J. Geophys. Res., 68,* in press, 1963.


(Manuscript received August 23, 1962.)



# The Scattering Behavior of the Moon at Wavelengths of 3.6, 68, and 784 Centimeters

J. V. EVANS AND G. H. PETTENGILL

*Lincoln Laboratory, Massachusetts Institute of Technology, Lexington*

*Abstract.* Experiments are described in which the scattering behavior of the moon has been investigated at wavelengths of 3.6 cm, 68 cm, and 7.84 meters. At 3.6 cm some 14 per cent of the surface appears to be covered by structure of the order of the wavelength in size, whereas at 68 cm only 8 per cent of the surface is this rough. The bulk of the surface appears to be smooth and undulating and describable by means of an exponential law for the lateral correlation of surface height. The mean gradient is found to vary, the wavelength being about 1 in 11 for points spaced by 68 cm and 1 in 7 for points spaced 3.6 cm. Interpreting these results to obtain a value for the reflection coefficient is complicated by the ability of the surface to scatter either more or less favorably than a perfectly smooth spherical surface. The best value that can be obtained from the radar results for the reflection coefficient is 6 per cent at 68 cm, which in turn yields a value for the dielectric constant of 2.8.

## 1. Introduction

The earliest radio-echo observations of the moon in 1946 [*DeWitt and Stodola,* 1949], served to show that radio signals reflected from the moon are subject to deep fading. Later it was established that the fading had two components [*Kerr and Shain,* 1951]. One component proved to be of ionospheric origin, namely, Faraday rotation [*Murray and Hargreaves,* 1954]. The other, faster component was shown to be caused by the apparent rotation of the moon as viewed by a terrestrial observer [*Browne et al.,* 1956; *Evans et al.,* 1959]. The Doppler broadening of the reflected signals was determined by *Evans* [1957] by measuring the rate of fading induced by the rotation. From this work, conducted at a wavelength of 2.5 meters, it was concluded that the moon reflected principally from a small region at the center of the visible disk. This 'limb dark' scattering behavior was independently discovered by *Trexler* [1958], who used a wavelength of 1.99 meters. *Yaplee et al.* [1958, 1959] and *Hey and Hughes* [1959] observed the same phenomenon at a wavelength of 10 cm. *Trexler* [1958], and later workers who followed him, conducted observations by transmitting short (approximately 1-msec) pulses and examining the distribution of echo power as a function of delay. The full lunar depth of the moon is 11.6 msec, but no echoes could be observed beyond about a 1-msec delay measured relative to the echo from the center of the moon. All these observers agreed that about 50 per cent of the reflected energy appeared to originate from a region at the center of the visible disk, having a radius of about one-tenth that of the moon.

Recently *Leadabrand et al.* [1960] and *Pettengill* [1960] showed that echoes can be observed out to the limbs of the moon if sufficient radar sensitivity is employed. This result stems from the fact that weak reflections appear to arise from all parts of the surface, though the predominant returns are from the center of the moon where the largest areas normal to the line-of-sight are to be found. *Pettengill and Henry* [1962a], who made observations at 68-cm wavelength, determined that 80 per cent of the total reflected energy was returned from these near regions, which appeared to scatter according to the law

$$\bar{P}(\phi) \propto \exp(-10.5 \sin\phi) \quad (1)$$

where $\bar{P}(\phi)$ is the average power reflected per unit element of surface along an incident and reflected ray path inclined at an angle $\phi$ to the normal to that element. This law was observed to hold over $7.5° < \phi < 60°$. The rest of the power was reflected from regions nearer the limbs (delay > 3.0 msec) and the scattering law observed for this component was

$$\bar{P}(\phi) \propto \cos^{3/2}\phi \quad (2)$$

*Hughes* [1960, 1961] has reported further

TABLE 1. The Parameters of the 3.6-cm Radar at Pleasanton, California

| | |
|---|---|
| Antenna | 60-foot diameter parabola with Cassegrain feed arrangement |
| Beamwidth (3 db one-way) | 0.14° |
| Polarization | Linear (both transmitted and received) |
| Antenna gain | 61 ± 1 db |
| Effective antenna aperture | 130 ± 35 meters² |
| Peak transmitter power | 12 ± 1/2 kw |
| Actual pulse length | 300 μsec |
| Pulse compression ratio | 10:1 |
| Over-all system temperature (when directed at the moon) | 225 ± 20°K |
| Receiver bandwidth | 30 kc/s approx. (i.e., matched to a 30-μsec pulse) |
| Over-all feeder losses | 1.5 ± 0.2 db |
| S/N improvement through video integration | Generally 18–20 db |

observations at a wavelength of 10 cm. No echoes could be detected beyond 1-msec delay, and hence the weak component could not be observed. The region near the center of the disk was found to scatter according to

$$\bar{P}(\phi) \propto \exp(-10.2\,\phi) \qquad (3)$$

over $3° < \phi < 14°$. From the similarity of (1) and (3), *Hughes* [1961] has concluded that the scattering of radio waves by the lunar surface is largely independent of their wavelength.

*Daniels* [1961] has undertaken a theoretical examination of the relationship between the roughness of the lunar surface, which was assumed to be everywhere the same and describable in statistical terms, and the measurements of the fading of the signals [*Evans and Pettengill*, 1962]. He concluded that if the height $h$ of the surface from the mean is normally distributed then the autocorrelation function $\rho(\epsilon)$, which specifies how the height varies as a function of distance $\epsilon$ over the surface, must be approximately given by

$$\rho(\epsilon) = 1 - \epsilon/\epsilon' + \cdots \quad \text{for small} \quad \epsilon/\epsilon' \qquad (4)$$

where $\epsilon'$ is the horizontal scale distance.

*Hughes* [1962] has drawn attention to the fact that such a surface would scatter differently at different wavelengths, and because it does not appear to do so he concludes that the assumption that the deviations of the surface height from the mean are normally distributed must be erroneous.

This paper reports a careful investigation of the scattering properties at three wavelengths, 3.6 cm, 68 cm, and 7.84 meters. The results show a clear wavelength dependence between 3.6 cm, 10 cm [*Hughes*, 1961], and 68 cm. However, no difference could be detected between the behavior at 68 cm and 7.84 meters.

In the following sections, the observations at 3.6 cm, 68 cm, and 7.84 meters will be described in this order, and some discussion will be given of the correspondence between these results and the existing theoretical work which relates them to a description of the lunar surface.

## 2. Observations at 3.6-cm Wavelength

*Method.* In these observations (as in the ones at 68-cm wavelength) the method employed has been to transmit short pulses and examine the distribution of echo power as a function of delay. Echoes from the moon are subject to deep fading as a consequence of the constructive and destructive interference from the many scattering elements distributed over the surface. Thus a single sweep of the radar time base shows a very irregular distribution of power as a function of delay, and many sweeps have to be averaged to determine the mean function for echo power versus delay, $\bar{P}(t)$. In this work the averaging was performed using an analog device containing 48 identical integrator channels. The receiver detector output was successively switched into these integrators for equal intervals of time, to cover the portion of the time-base occupied by the lunar echo. This process was repeated for periods of up to 10 minutes (i.e. $\sim 10^4$ sweeps). The pulse length employed for the transmitter was 30 μsec and the integration was carried out over intervals of 20, 100, 200, and 500 μsec per integrating channel.

*Equipment.* The radar equipment used for measurements at 3.6-cm wavelength is near Pleasanton, California, at a field site operated by MIT's Lincoln Laboratory. Though many details of the radar equipment and the integrator are novel and of interest in their own right, no description will be given here. Instead the parameters of the equipment are summarized in Table 1, and further details may be found in *Evans* [1962*a*].

One feature of the system that does deserve comment is the antenna. This is a parabola, 60 feet in diameter, having a Cassegrain feed system. The half-power beamwidth of the antenna is 0.14°, which is substantially less than the angular diameter of the moon (0.5°). In principle this should provide a means of examining different parts of the lunar surface to determine whether or not they reflect in the same fashion. Unfortunately this ability is partly destroyed by the asymmetrical radiation pattern of the instrument. By placing a transmitter at an elevated site some distance from the antenna (on Mount Diablo) the antenna pattern has been determined and is presented in Figure 1 as a series of isophotes at 3-db intervals. The pattern shown in Figure 1 may not represent the true distribution of the transmitted signal over the moon because ground reflections may have been present during the pattern measurements, or the pattern may have changed with the elevation of the beam owing to the changing gravitational load on the structure. Radio stars have not yet been observed with sufficient precision to check Figure 1 in great detail.



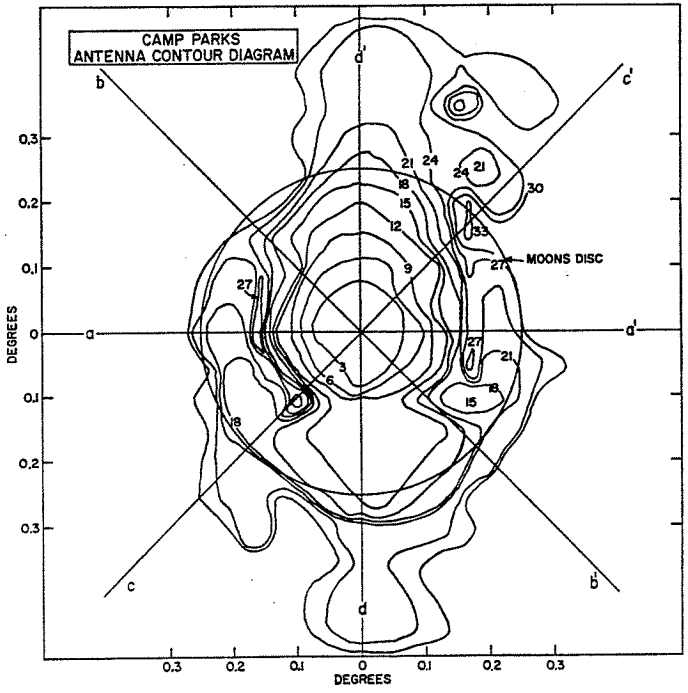


Fig. 1. The intensity contours of the antenna employed for observations at 3.6-cm wavelength. These contours, in 3-db intervals, indicate the manner in which the transmitter power is distributed across the moon's disk.

*Observations.* The antenna was steered by a digital electronic control system to point toward the center of the moon continuously. The average distribution of echo power with range delay could then be established by continuing the integration process for periods of 5 or 10 minutes for data samples at increments of 20, 100, 200, and 500 μsec. The motion of the echo on the time base due to the relative motion of the earth and the moon was compensated by shifting the position of the integration intervals at a linear rate by means of electronic timing circuits. This range compensation was accomplished in a series of 'jumps,' each of 10 μsec, and hence was unsuited for observations where the narrowest delay increments (20 μsec) were employed. The

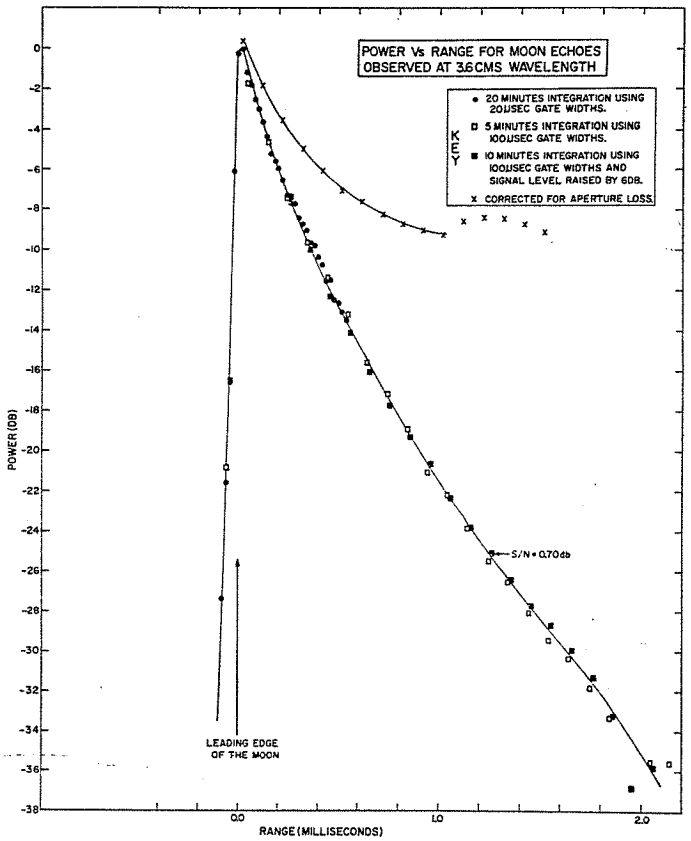


Fig. 2. The echo power as a function of range delay observed at 3.6-cm wavelength when the antenna was directed at the center of the moon. The crosses represent the curve of echo power versus delay obtained when the line through the experimental points is corrected for the effect of the antenna (Figure 3).

20-μsec measurements were, therefore, made only near meridian transit, when the motion of the echo was very small ($< \pm 5$ μsec) for a brief period. Echoes were measured on September 6–9 and 11, and results are summarized in a composite plot of power versus delay in Figure 2.

It can be seen from Figure 2 that no echoes could be detected beyond 2-msec delay. This is largely a consequence of the narrow beam of the antenna. A correction diagram indicating the effect of the antenna (Figure 3) has been obtained in the following way. The area in square degrees inside each isophote in Figure 1 was determined by means of a planimeter, and was then equated to the area of an equivalent disk. The idealized antenna pattern obtained from these measurements was converted to a power versus delay plot. The curve shown in Figure 3 represents the sensitivity function of the antenna for radar observations of the center of the moon. When the experimental results presented in Figure 2 are corrected by using the curve of Figure 3, the correction factors rapidly get very large and it is believed that they are unreliable beyond about 1-msec delay. Thus the corrections have been applied at less than this delay only, and the curve drawn through the crosses in Figure 2 represents the brightness distribution over the moon's surface as it might be observed using a broadbeam antenna.



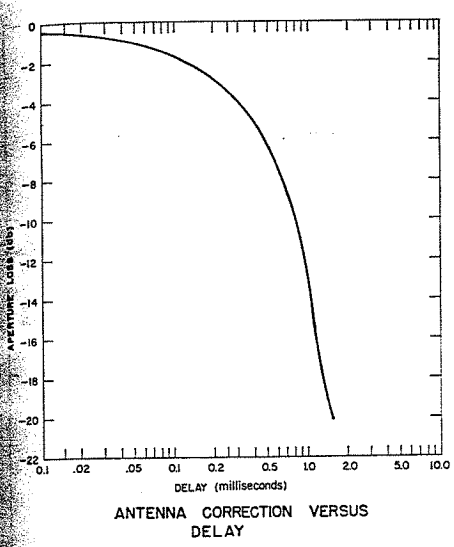


Fig. 3. The antenna correction factor as a function of range delay. This diagram shows the weighting of the radar antenna pattern (Figure 1) to echoes from different range delays. This curve was obtained from Figure 1 by using a planimeter to obtain the area within each contour.

To obtain the distribution of echo power at greater ranges it was necessary to direct the beam away from the center of the moon. Figure 4 shows one of two positions employed, namely a distance of one beamwidth (0.14°) from center. Observations were made in all four quadrants by driving the antenna off center either in azimuth (right or left) or in elevation (high or low) by means of manual controls. These controls introduce an integral number of 0.02° displacements between the beam and the on-center position called for by the electronic control system.

A correction diagram for the effect of the antenna in this offset position was obtained from Figure 4 by computing the amount of projected area on a given range delay contour that falls inside a given intensity contour, and then by weighting these areas and summing.

Measurements were also made with the antenna displaced from center by 0.22° (approximately one and a half beamwidths). As before, echoes were measured in all four quadrants, and a mean of the plots of the echo power observed as a function of delay obtained in these quadrants was taken as representing the average scattering behavior. Another correction diagram was prepared, and the corrected results for all three positions of the antenna with respect to the moon's center are presented in Figure 5. Where the measurements overlap they appear to be in good agreement, indicating no serious error in the procedure employed for correcting for the effects of the antenna. A more detailed account of the experimental work described above may be found in *Evans* [1962*a*].

### 3. Observations at 68-cm Wavelength

*Method.* Short-pulse measurements have been made at this wavelength using (*a*) 30-μsec pulses to achieve a resolution similar to that obtained at 3.6-cm wavelength, and (*b*) 12-μsec pulses to obtain a resolution comparable to that achieved by *Hughes* [1961] at 10-cm wavelength. The antenna used in this work has a beam wider than the moon (2.1°), and the difference in equipment sensitivity between echoes from the center and limb regions is about 1 db. As the measured echo intensities from these two regions differ by about 40 db, this small correction has been neglected.

*Equipment.* The Millstone Hill radar facility in Westford, Massachusetts, was used; the parameters of the radar are listed in Table 2, and further details can be found in *Pettengill and Kraft* [1958] or *Arthur et al.* [1961]. Some comments concerning these measurements are in order. Two methods of averaging were employed. In one the analog integrator described earlier was used, whereas in the other a digital voltmeter sampled the echo, then a digital (CG-24) computer was used for summation. The first method has the advantage of fine range resolution (10-μsec minimum) but has a limited number of channels (48 in total) and an accuracy of about ±2 per cent. The second method has the advantage of absolute stability and freedom from drift, but cannot be used to sample range intervals closer than 200 μsec apart. Circularly polarized waves were transmitted and received to overcome the slow period fading caused by Faraday rotation in the earth's ionosphere. (Note that Faraday rotation was negligible at all times for the 3.6-cm wavelength described in the preceding section.)

*Observations (30-μsec pulses).* For measurements on November 10 and December 6, 1961,

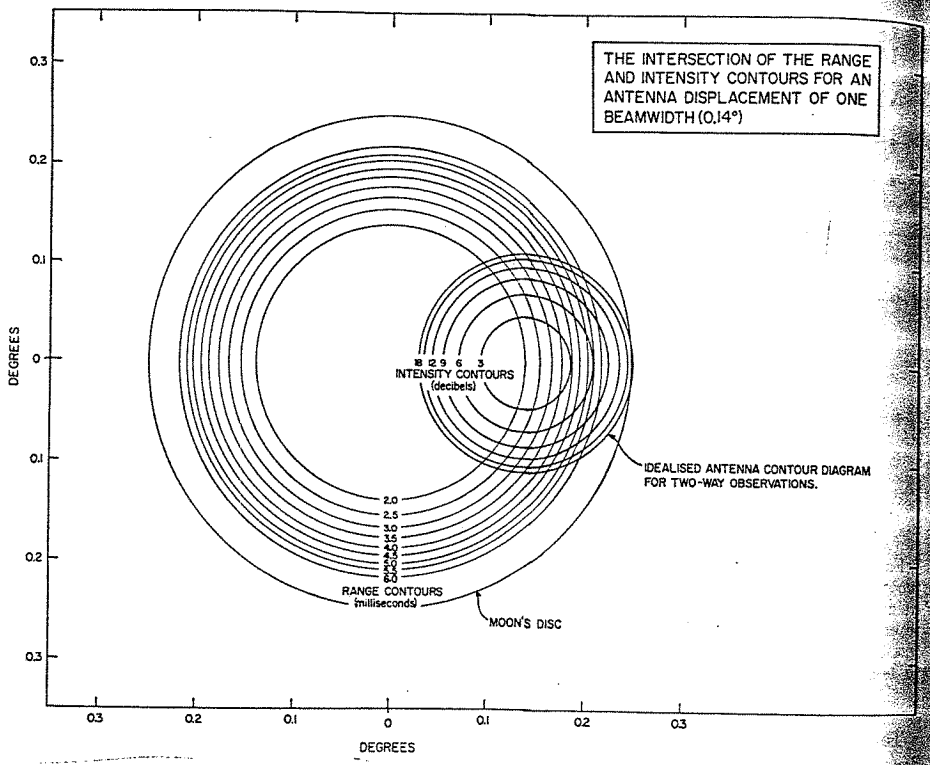


Fig. 4. This diagram shows, in plan form, the intersection of the range delay contours and the idealized antenna contour diagram when the 3.6-cm antenna was directed one beamwidth (0.14°) from the center of the moon. Because the echo intensity is proportional to the *projected* area of the surface inside each contour, it is possible to compute a new antenna correction diagram.

pulses of 65-$\mu$sec duration were used to establish the accuracy of the analog integration system. These measurements could be compared directly with the earlier ones by *Pettengill and Henry* [1962*a*] in which the digital integration system was used. This work served to show that the analog system (which had been used for the 3.6-cm work) was of accuracy comparable to the digital system, and was better able to resolve the distribution of power in the region of the peak of the echo, corresponding to echoes from the center of the disk.

On December 6, 1961, using 30-$\mu$sec transmitter pulses and a receiver bandwidth of 48 kc/s, the measurements were made entirely by means of the analog integration system with gate widths of 20, 100, and 250 $\mu$sec. The results of this work are shown in Figure 6, together with the results obtained previously at 3.6 cm. The distribution of echo power with delay is the same as that observed by *Pettengill and Henry* [1962*a*] for delays $>1$ msec. However the use of a shorter pulse together with finer sampling intervals yields a better resolution of the echo power in the vicinity of the peak. *Hughes* [1961] used 5-$\mu$sec transmitter pulses, but a resolution in delay of only 20 $\mu$sec. Thus it is probable that the over-all resolution of his system was about twice that employed in these 3.6- and 68-cm measurements, and hence a strict comparison of the results in the region 0–30 $\mu$sec would be improper. Figure 7 provides a comparison of the results for delays $>10$ $\mu$sec, and the wavelength dependence of the scattering is clearly evident.

*Observations (12-$\mu$sec pulses).* On January 26, 1962, observations were made using 12-$\mu$sec



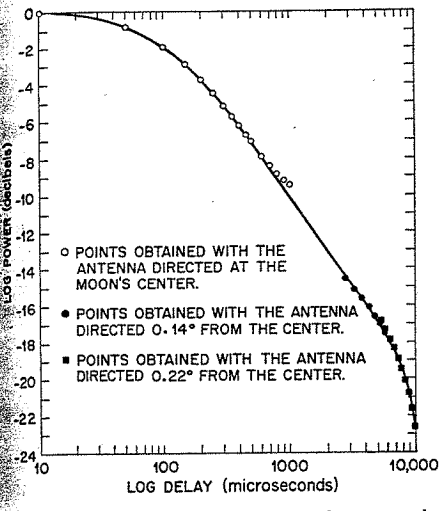


Fig. 5. The echo intensity versus log range delay observed at 3.6 cm. This diagram combines the results obtained for all three positions of the antenna with respect to the moon's center.

transmitter pulses and a receiver bandwidth of 115 kc/s. The analog integration equipment was again used, but this time only the region of delays up to 750 $\mu$sec was explored. Gate widths of 10, 20, and 50 $\mu$sec were used; the resulting composite curve and the average points obtained by *Hughes* [1961] are shown in Figure 8. It is believed that the resolution in range achieved in this work is at least as good as Hughes', and hence these two curves accurately indicate the different behavior of the moon at the two wavelengths.

To explore the distribution of echo power beyond 750-$\mu$sec delay, the digital integration system was used. Because of the limited dynamic range of the digital voltmeter, it was necessary to make two sets of measurements. On January 26 the region of delays 2–12 msec was examined using a resolution of 250 $\mu$sec. Later (on April 3, 1962) the region 0–3 msec was explored by means of a different experimental arrangement that permitted the range changes of the echo to be compensated during the integration process. Also on April 3 a resolution of 100 $\mu$sec was achieved by interlacing successive time-base sweeps sampled at 200-$\mu$sec intervals. These results are presented in Figure 9 and have been combined

TABLE 2. The Parameters of the 68-cm Radar at Millstone Hill, Massachusetts

| | |
|---|---|
| Antenna | 84-foot diameter parabola |
| Beamwidth (3 db one-way) | 2.1° |
| Polarization | Right circular (transmitted) left circular (received) |
| Antenna gain | 37.5 ± 0.5 db |
| Effective antenna aperture | 208 ± 25 meters² |
| Peak transmitter power | 2.5 ± 0.1 Mw |
| Pulse length | 12, 30, or 65 $\mu$sec |
| Over-all system temperature (when directed at the moon) | ≈300°K (measured daily) |
| Receiver bandwidth | 48 kc/s for 30- and 65-$\mu$sec pulses; 115 kc/s for 12-$\mu$sec pulses |
| Over-all feeder losses | 2 db |
| S/N improvement through video integration | Generally 20 db |

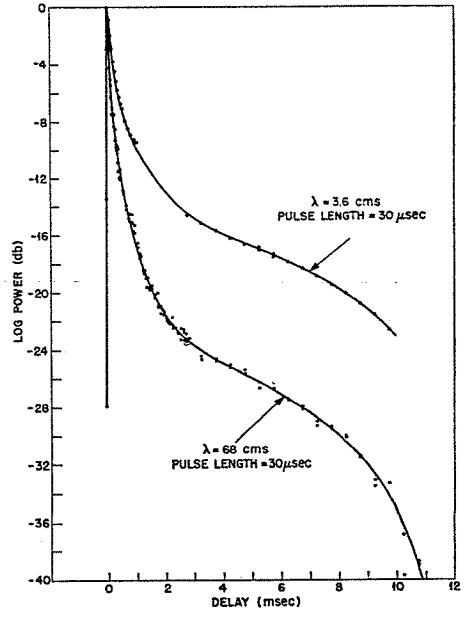


Fig. 6. The average echo power reflected by the moon $\bar{P}(t)$ as a function of delay measured with respect to the point closest to the radar. The 68-cm results were obtained using the same methods of averaging as were employed to obtain the 3.6-cm results (Figure 5).

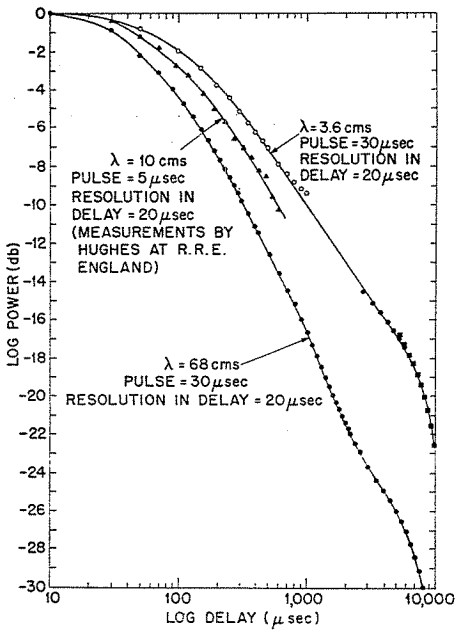


Fig. 7. The average echo power observed at 3.6- and 68-cm wavelength (Figure 6) shown together with results obtained by *Hughes* [1961] at 10 cm. The results have been normalized at the origin and plotted as a function of log range delay to demonstrate their wavelength dependence.

with those shown in Figure 8 to give the composite plot contained in Figure 10. The curve showing the depolarized component of the signals will be discussed next.

*Polarization measurements.* The measurements at 68 cm reported in the previous sections were all made when right circularly polarized waves were transmitted and left circularly polarized waves were received. The use of circular polarization, as distinct from linear, is advantageous in that it eliminates the undesirable effects of ionospheric Faraday rotation. The amount of depolarization of the signals by both transmitting and receiving right circularly polarized waves has been determined. Figure 11 (and in gross terms, Figure 10) shows the results of measurements made on April 3 with 200-μsec transmitter pulses, using two interlaced timebase sweeps to obtain a resolution of 100 μsec. It can be seen in Figure 11 that although there are significant departures from a smooth curve the intensity is approximately given by

$$\bar{P}(\phi) \propto \cos\phi \qquad (5)$$

The departures from this smooth curve are of interest in that they show that the moon is not wholly homogeneous. Similar, though smaller, departures are regularly observed in the polarized returns, particularly near 4-msec delay. The location of these irregular regions can be determined by 'mapping' the power into both range and Doppler coordinates [*Pettengill*, 1960], and the bright region at 4-msec delay is believed to be associated with the crater Tycho [*Pettengill and Henry*, 1962*b*].

The absolute levels of the echo intensity in Figures 9 and 11 were determined by including in the processing a pulse of wideband noise which was injected into the receiver on each sweep of the timebase. When we allow for the ratio of the pulse widths in these two experiments and the higher feedline loss (1 db) for reception of left-circular waves as opposed to right-circular, the relative intensity of the two components appears as shown in Figure 10. The amount of polarization $p(t)$ of the signals can be obtained at each delay from the ratio of the two curves. If $L_{P(t)}$ is the intensity of the left-hand (polarized) component and $R_{P(t)}$ that of the right-hand (depolarized) component, we have

$$p(t) = \frac{L_{P(t)} - R_{P(t)}}{L_{P(t)} + R_{P(t)}} \qquad (6)$$

The value of $p(t)$ (expressed as a percentage) obtained from Figure 10 is given in Figure 12. The points obtained earlier by *Pettengill and Henry* [1962*a*] also appear in Figure 10. The results of the two experiments agree reasonably well, and indicate that the returns from the leading edge of the moon are almost completely polarized. The percentage of polarization falls almost linearly to a value of about 65 per cent at a delay of 3 msec. Beyond this point there is only a small further decrease, the value observed near the limbs being approximately 40 per cent. Further details of the experimental work conducted at 68-cm wavelength have been given by *Evans* [1962*c*].

## 4. Observations at 7.84 Meters

*Method.* At wavelengths longer than 68 cm echoes have not been observed with sufficient



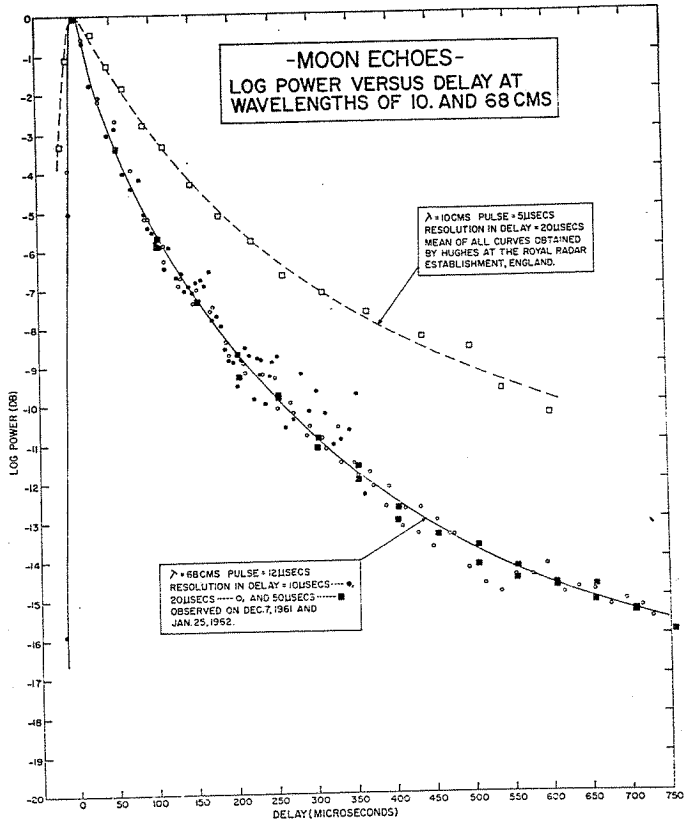


Fig. 8. High resolution measurements of $\bar{P}(t)$ at 68-cm wavelength for the region closest to the radar. Also shown are *Hughes'* [1961] measurements.

precision to indicate any wavelength dependence [*Hughes*, 1961]. Accordingly, lunar echo observations were made using the Lincoln Laboratory Solar Radar near El Campo, Texas [*Abel et al.*, 1961]. This radar equipment transmits a CW signal, and hence could not be used for the type of measurements described previously. For this reason a different approach was adopted.

*Hagfors* [1961] has shown that if two sine waves are reflected from the moon they will fade either similarly or independently depending upon their frequency separation $\Delta f$. The cross-correlation function $\gamma(\Delta f)$, which describes the correlation between echo amplitudes at the two frequencies, is related to the average echo power versus delay function, $\bar{P}(t)$, by

$$\gamma(\Delta f) = [\text{Fourier cosine transform of } \bar{P}(t)]^2 \qquad (7)$$

if the two detectors have square law characteristics [*Evans and Pettengill*, 1962]. This result (equation 7) depends only on the assumption that the echoes resemble narrow-band Gaussian noise, and because the distribution of echo amplitudes is found to follow the Rayleigh law [*Browne et al.*, 1956] there seems no reason to doubt its validity. Measurements of $\gamma(\Delta f)$ have been performed at a wavelength of 68 cm by *Ingalls et al.* [1961]; thus the scattering behavior at 7.84 meters and 68 cm could be compared by repeating the earlier measurements at the longer wavelength.

*Equipment.* The El Campo solar radar operates at a frequency of 38.25 Mc/s (λ = 7.84 meters) and has been built and operated by MIT's Lincoln Laboratory principally to obtain radar echoes from the solar corona [*Abel et al.*,

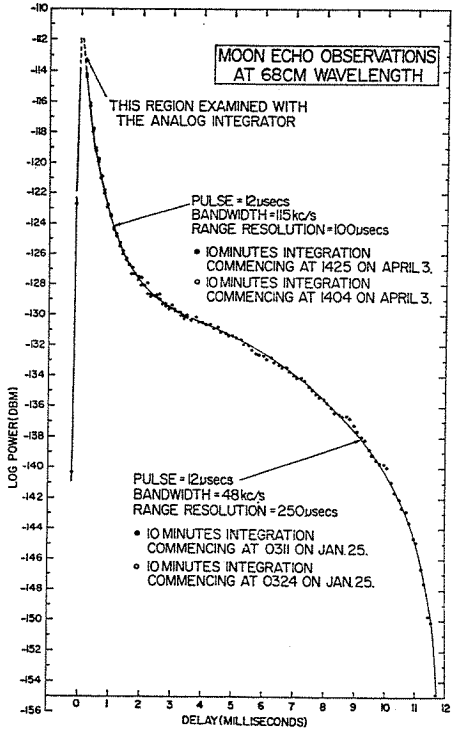


Fig. 9. The average echo intensity as a function of range delay obtained by employing a digital method of integration.

1961]. The parameters of the transmitting and receiving equipment are listed in Table 3. The use of a CW transmission necessitated a receiving site some distance from the transmitter, and for this purpose Millstone Hill was employed. The transmitter was phase-modulated in a manner that caused equal amounts of power to be radiated at three frequencies (the carrier and immediate side bands). Two receivers were employed, each having a passband of 25 cps. One receiver was tuned to the carrier frequency and the other to one of the side bands. The output of the two receivers was sampled simultaneously by means of two identical digital voltmeters at a rate of 20 cps. These samples were converted to numbers taken via the CG 24 computer and stored on digital tape. Frequency separations of less than 100 cps could not successfully be used because of coupling between the receivers and the unwanted signals. Experience at 68 cm showed that at frequencies higher than 10 kc/s the correlation has essentially disappeared.

*Observations.* The observations reported here were made during the period January 31 to February 3, 1962. The duration of any one day's measurements was limited to about 50 minutes by the narrow east-west extent of the transmitting antenna. Consequently on each day only four 12-minute runs were attempted using different separations $\Delta f$. Although a circularly polarized receiving antenna was employed, some residual Faraday fading having a quasi-period of the order of 4 minutes was evident on most records. The digital samples stored on magnetic tape were used first to provide a 'smoothed' sample of the receiver voltage every 1/4 second by means of a computer program that simulated the behavior of a low-pass filter. These 1/4 second samples were then used in the computation of the cross-correlation function $\gamma(\Delta f)$ (again using the CG 24 computer). A cross-correlation coefficient was obtained for each one-minute interval in each of the runs. The mean cross-correlation coefficient for each run was then obtained. By breaking the runs into intervals shorter than the Faraday fading, and cross-correlating these separately, we hoped to overcome the unwanted changes in the mean signal level which would alter the correlation observed. However, it is possible that ionospheric scintillations might also have existed that were not completely correlated at the two frequencies.

The results of this work are shown in Figure 13, together with the earlier results published by Ingalls et al. for 68-cm wavelength. The errors shown are estimated errors obtained from the scatter of the 12 values obtained for each run. The curve of Figure 13 is the Fourier cosine transform of $\bar{P}(t)$ (equation 7) and hence must largely be controlled by the strong echoes from the central region. To the accuracy of the experimental points there seems no difference between the results at the two wavelengths. This conclusion should, however, be regarded as preliminary, and more experiments are planned which should shed further light on the behavior at this wavelength. In particular the pulse method is probably insensitive to the presence or absence of the weak echoes from the outer regions, and, even if the central regions behave in the same fashion at the two wavelengths, it



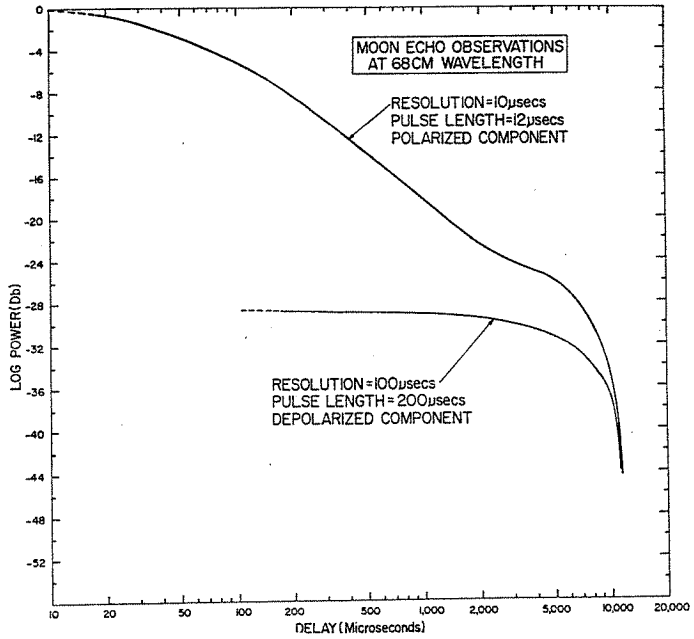


Fig. 10. The high resolution curve for $\bar{P}(t)$ obtained by combining the results shown in Figures 8 and 9. Also shown on a relative intensity scale are the results of the depolarized measurements (Figure 11).

need not follow that the amount of energy returned from the other regions will be the same.

## 5. The Angular Power Spectrum $\bar{P}(\phi)$

*Introduction.* The relationship between the delay $t$ and the angle of incidence $\phi$ is shown in Figure 14. It is clear that a given range delay $t$ corresponds to an annulus on the surface for which there is a single value of $\phi$. This property of a sphere has been recognized by many workers, and enables echo power plotted as a function of delay $\bar{P}(t)$ to be replotted to power as a function of angle $\bar{P}(\phi)$ since

$$\phi = \cos^{-1}(1 - ct/2a) \tag{8}$$

The resulting distribution of echo intensity with angle of incidence $\bar{P}(\phi)$ we shall call the angular power spectrum. The actual area of the surface illuminated by a pulse of duration $\tau$ seconds is $\pi a c\tau$, i.e., independent of the delay $t$, and $\bar{P}(\phi)$ states the angular distribution of the echo power per unit element of the surface. However, the echo intensity depends on the projected surface area which varies with $\phi$ as $\cos\phi$. Thus we should expect a uniformly bright surface to obey a law

$$\bar{P}(t) \propto (1 - ct/2a) \tag{9}$$

or

$$\bar{P}(\phi) \propto \cos\phi \tag{5}$$

If the assumption is made that the lunar surface, when sampled over areas of the order of kilometers across,[1] consists on the average of the same kind of materials and has the same statistical surface roughness everywhere, then the angular power spectrum $\bar{P}(\phi)$ may be taken as representing the scattering characteristics of any element of the surface.

*3.6-cm observations.* When the points corresponding to $\lambda = 3.6$ cm shown in Figure 6 are plotted as a function of $\cos\phi$, Figure 15 is

[1] A 10-μsec transmitted pulse illuminates an annulus on the surface of the moon having an area of about 8000 km².

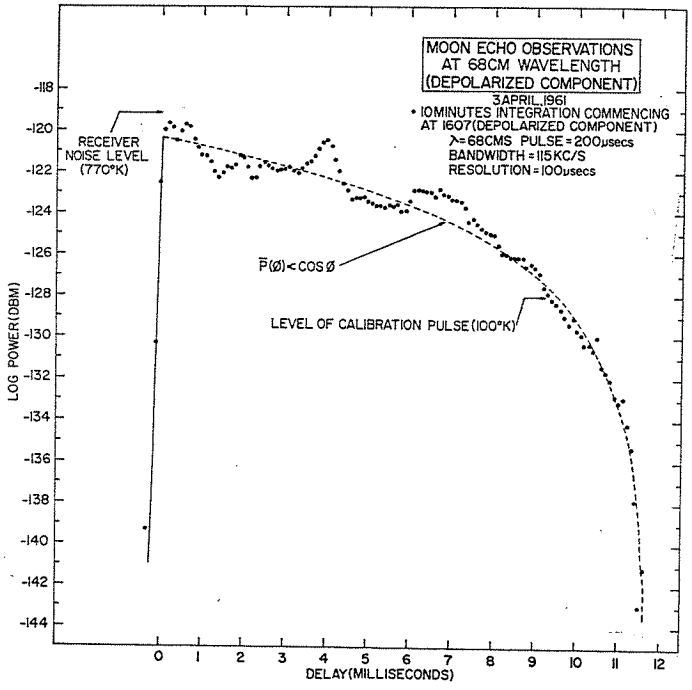


Fig. 11. The average echo intensity versus range delay curve for the depolarized component of the signals. The dotted curve indicates the expected behavior for a uniformly bright moon. The departure of the experimental points from the dotted curve is believed to be significant, and the peak observed at 4 msec delay is thought to be associated with the crater Tycho. [*Pettengill and Henry*, 1962*b*].

obtained. It can be seen that over the range $55° < \phi < 90°$ the law

$$\bar{P}(\phi) \propto \cos \phi \qquad (5)$$

fits the results extremely well, indicating that the limb region is uniformly bright. If this component is subtracted from the total power, we should expect by analogy with results of *Pettengill and Henry* [1962*a*] and *Hughes* [1961] to be left with a component that would fit some simple law of the form $\bar{P}(\phi) \propto \exp(-A \sin \phi)$. The logarithm of the remainder has, therefore, been plotted against $\sin \phi$ in Figure 16. It can be seen that the function $\exp -7.1 \sin \phi$ fits the results near the origin $5° < \phi < 18°$ but not elsewhere.

*68-cm observations (30-μsec pulses).* *Pettengill and Henry* [1962*a*] observed that in the regions near the limbs ($60° < \phi < 90°$) the angular power spectrum took the form

$$P(\phi) \propto \cos^{3/2} \phi \qquad (2)$$

The present work supports this conclusion. The remainder has been plotted as a function of $\sin \phi$ in Figure 17. No simple law fits the points over the whole range of $\sin \phi$. Figure 17 also shows the theoretical curve obtained by *Daniels* [1961] and it would appear that the two curves are in fairly good agreement. A small region near the origin ($5° < \phi < 12°$) can be made to fit the law

$$P(\phi) \propto \exp(-12.5 \sin \phi) \qquad (10)$$

as shown in Figure 18. No attempt has been made to correct the results in the manner employed by Hughes. Instead additional measurements were made using 12-μsec pulses which are reported in the next section. Pulses shorter than 30 μsec could not be employed at 3.6-cm wavelength at the time these observations were made.

*68-cm observations (12-μsec pulses).* When the results given in Figure 10 are plotted as a function of $\cos \phi$ (Figure 19) it is again found that over a substantial range of angles ($45° < \phi < 80°$) the law

$$\bar{P}(\phi) \propto \cos^{3/2} \phi \qquad (2)$$



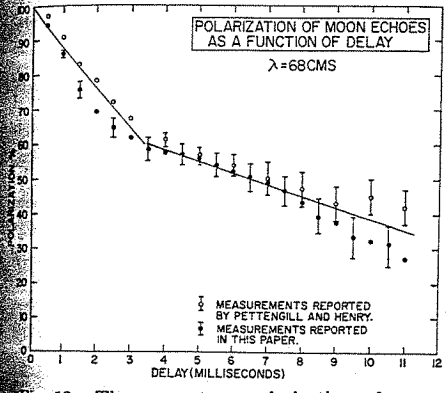


Fig. 12. The percentage polarization of moon echoes as a function of range delay observed at 68-cm wavelength. These values were computed from the results shown in Figure 10 by means of the expression given in (6). The earlier values obtained by *Pettengill and Henry* [1962*a*] are also shown.

is observed. However at the limbs ($\phi > 80°$) the law

$$\bar{P}(\phi) \propto \cos \phi \qquad (5)$$

seems a better fit to the experimental points. This law indicates that the limb region is uniformly bright, whereas over the range $45° < \phi < 80°$ there is some limb darkening. It is possible in view of the $\cos \phi$ dependence

TABLE 3. Parameters of the Equipment

| | |
|---|---|
| 7.84-meter radar at El Campo, Texas | |
| Transmitting antenna | Phased array of dipoles 1750′ north-south by 110′ east-west |
| Beamwidth | 15° east-west by 0.75° north-south |
| Polarization | Linear |
| Antenna gain | 34 ± 2 db |
| Transmitter power | ≈400 kw (measured daily) |
| Receiving system at Millstone Hill, Mass. | |
| Receiving antenna | Two 3-element Yagi antennas mounted in orthogonal planes |
| Beamwidth (3 db) | ∼±50° |
| Polarization | Left or right circular |
| Antenna gain | ≈9 db |
| Over-all system temperature | ≈20,000°K (set by the sky background) |
| Receiver bandwidth | 25 cps |

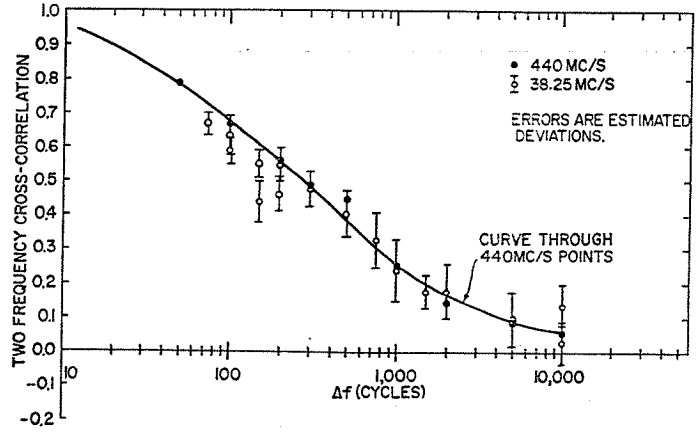


Fig. 13. The values for the normalized correlation between the amplitudes of two radio waves separated in frequency by $\Delta f$ cps after reflection by the moon. This function is related to $\bar{P}(t)$ by a Fourier transformation. The measurements shown for 440 Mc/s (68 cm) are those of *Ingalls et al.* [1961] and those for 38.25 Mc/s (7.84 meters) appear to indicate little change in the reflection properties at this wavelength.

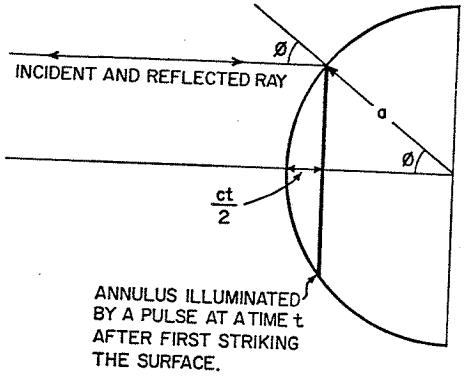


Fig. 14. The relation between the range delay $t$ and the angle of incidence $\phi$ of the radio waves.

observed at the limbs that the law $\cos^{3/2}\phi$ observed elsewhere represents a combination of scattering dependent both on $\cos\phi$ (Euler, or approximately Lommel-Seeliger) and $\cos^2\phi$ (Lambert).

When these diffuse components have been subtracted out, and the power again plotted as a function of $\sin\phi$, the results show no simple relation of the form $\bar{P}(\phi) \propto \exp(-A\sin\phi)$ suggested by *Hughes* [1961], though a small region near the origin ($3° < \phi < 9°$) will fit a law

$$\bar{P}(\phi) \propto \exp(-15.3\sin\phi) \qquad (11)$$

as may be seen in Figure 20.

*68-cm depolarized component.* In Figure 11 we saw that the depolarized component follows quite closely the law

$$\bar{P}(\phi) \propto \cos\phi \qquad (5)$$

indicating that in 'depolarized light' the surface appears uniformly bright.

*General laws for the quasi-specular component.* A simple empirical law has been sought that would provide an approximate fit to the quasi-specular component at 3.6 and 68 cm over a wide range of angles $\phi$. The only law that came close to fitting the experimental points obtained at both wavelengths was

$$\bar{P}(\phi) \propto \frac{1}{1 + b\phi^2} \qquad (12)$$

$b = 460$ $\quad \lambda = 68$ cm

$b = 50$ $\quad \lambda = 3.6$ cm

The experimental results and this empirical law are compared in Figure 21.

*Wavelength dependence.* The presence or absence of wavelength dependence in the scattering behavior can be established only when echoes are measured at different wavelengths using comparable resolution. For example, measurements made at 68 cm using 65-$\mu$sec pulses [*Pettengill and Henry*, 1962*a*] indicated that a law of the form $\bar{P}(\phi) \propto \exp(-A\sin\phi)$ would fit the results over a range of angles $7.5 < \phi < 60°$ when the exponent $A$ was 10.5. However, when the measurements were repeated using 30-$\mu$sec pulses and finer sampling intervals (this paper), only the power in the region $5° < \phi < 12°$ would fit such a law, and the value obtained for $A$ was 12.5. Finally, for measurements made with 12-$\mu$sec pulses and still finer sampling intervals, this law seemed to fit only over the region $3° < \phi < 9°$ with a value for $A$ of 15.3. We attribute this behavior

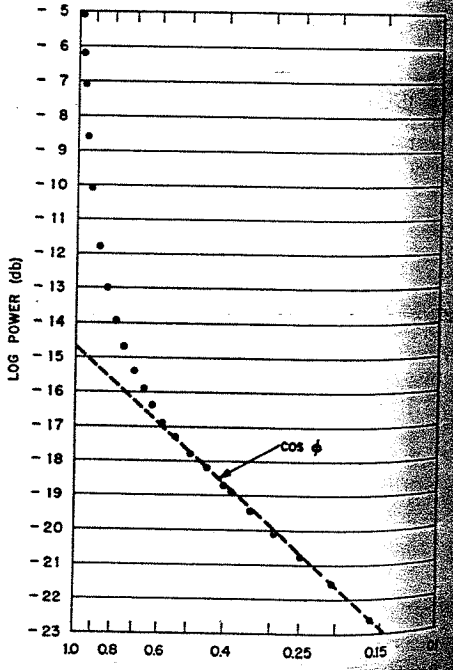


Fig. 15. The values for the echo intensity at 3.6 cm shown in Figure 5 are here replotted as a function of log $\cos\phi$.



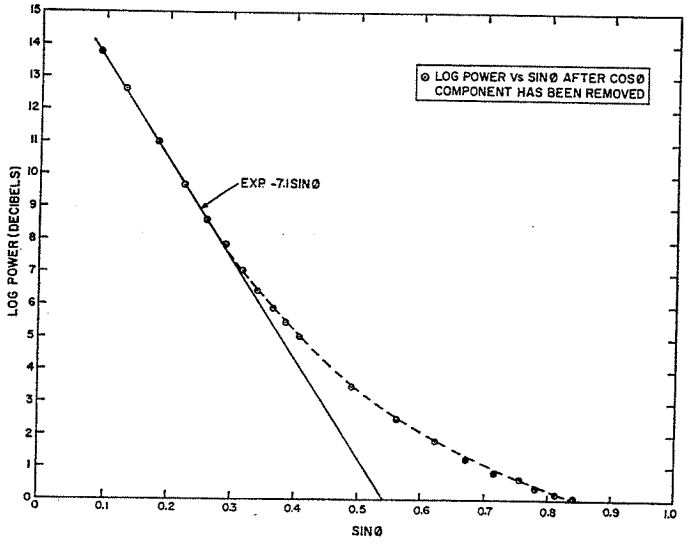


Fig. 16. The variation of the echo intensity at 3.6 cm as a function of $\sin\phi$ when the component that obeys the $\cos\phi$ law (Figure 15) has been removed.

imply to the improved resolution afforded by ing shorter pulses and conclude, in contrast to *ughes* [1961], that the law $\bar{P}(\phi) \propto \exp(-A$ $\phi)$ has no general validity.

Measurements made with 30-$\mu$sec pulses can used to compare the scattering behavior at 6- and 68-cm wavelengths. For $\phi \leq 12°$ we nd

$\phi) \propto \exp(-7.1\sin\phi)$ at 3.6 cm (13)

$\phi) \propto \exp(-12.5\sin\phi)$ at 68 cm (10)

he measurements made at 68 cm with 12-$\mu$sec ulses have a resolution comparable with those ade by Hughes at 10 cm, and a proper com-rison of the behavior at these two wavelengths the region $3° < \phi < 9°$ is contained in

$\phi) \propto \exp(-10.2\phi)$ at 10 cm (3)

$\phi) \propto \exp(-15.3\sin\phi)$ at 68 cm (11)

## Total Reflected Power and Dielectric Constant of the Surface

he data presented in Figure 6 have been malized at the origin. The total reflected er can be obtained by integrating the area r the curve for $\bar{P}(t)$. In this way the radar s section of the moon can be determined, given a knowledge of the equipment parameters (Tables 1 and 2). When expressed as a percentage of the physical cross section presented by the moon's disk ($\pi a^2$) the value obtained at 3.6 cm is $2 \pm 1$ per cent and at 68 cm is $7 \pm 1$ per cent. The 68-cm value is close to that observed by *Fricker et al.* [1960]. The low value obtained at 3.6 cm is in conflict with a value of $7 \pm 2\frac{1}{2}$ per cent obtained at the same wave-

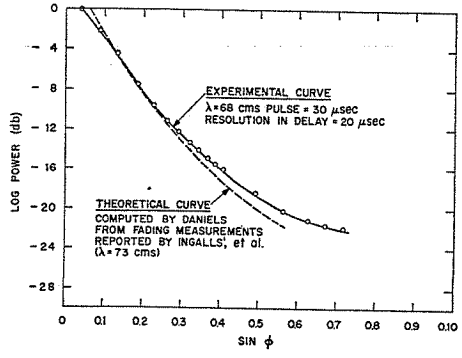


Fig. 17. The variation of the echo intensity at 68 cm shown in Figure 6 with $\sin\phi$. A component that appears to obey a $P(\phi) \propto \cos^{3/2}\phi$ has been removed. The results of theoretical calculations by *Daniels* [1961] are shown for comparison.

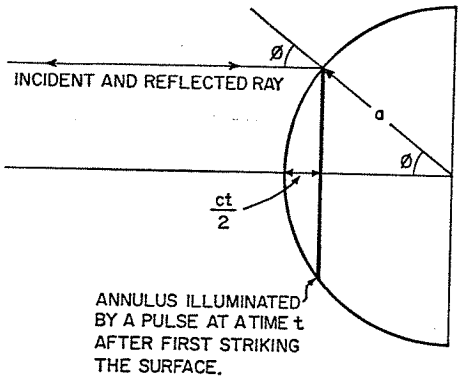


Fig. 14. The relation between the range delay $t$ and the angle of incidence $\phi$ of the radio waves.

observed at the limbs that the law $\cos^{3/2}\phi$ observed elsewhere represents a combination of scattering dependent both on $\cos\phi$ (Euler, or approximately Lommel-Seeliger) and $\cos^2\phi$ (Lambert).

When these diffuse components have been subtracted out, and the power again plotted as a function of $\sin\phi$, the results show no simple relation of the form $\bar{P}(\phi) \propto \exp(-A\sin\phi)$ suggested by *Hughes* [1961], though a small region near the origin ($3° < \phi < 9°$) will fit a law

$$\bar{P}(\phi) \propto \exp(-15.3\sin\phi) \qquad (11)$$

as may be seen in Figure 20.

*68-cm depolarized component.* In Figure 11 we saw that the depolarized component follows quite closely the law

$$\bar{P}(\phi) \propto \cos\phi \qquad (5)$$

indicating that in 'depolarized light' the surface appears uniformly bright.

*General laws for the quasi-specular component.* A simple empirical law has been sought that would provide an approximate fit to the quasi-specular component at 3.6 and 68 cm over a wide range of angles $\phi$. The only law that came close to fitting the experimental points obtained at both wavelengths was

$$\bar{P}(\phi) \propto \frac{1}{1 + b\phi^2} \qquad (12)$$

$b = 460 \qquad \lambda = 68$ cm

$b = 50 \qquad \lambda = 3.6$ cm

The experimental results and this empirical law are compared in Figure 21.

*Wavelength dependence.* The presence of a wavelength dependence in the scattering behavior can be established only when echoes are measured at different wavelengths using comparable resolution. For example, measurements made at 68 cm using 65-$\mu$sec pulses [*Pettengill and Henry*, 1962*a*] indicated that a law of the form $\bar{P}(\phi) \propto \exp(-A\sin\phi)$ would fit the results over a range of angles $7.5 < \phi < 60°$ when the exponent $A$ was 10.5. However, when the measurements were repeated using 30-$\mu$sec pulses and finer sampling intervals (this paper), only the power in the region $5° < \phi < 12°$ would fit such a law, and the value obtained for $A$ was 12.5. Finally, for measurements made with 12-$\mu$sec pulses and still finer sampling intervals, this law seemed to fit only over the region $3° < \phi < 9°$ with a value for $A$ of 15.3. We attribute this behavior

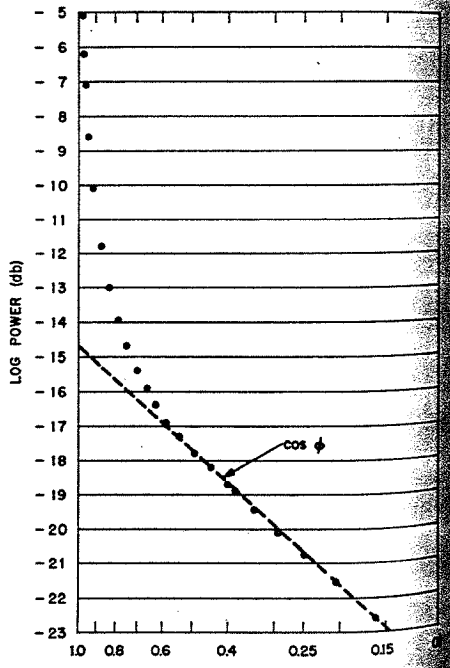


Fig. 15. The values for the echo intensity at 3.6 cm shown in Figure 5 are here replotted as a function of log cos $\phi$.



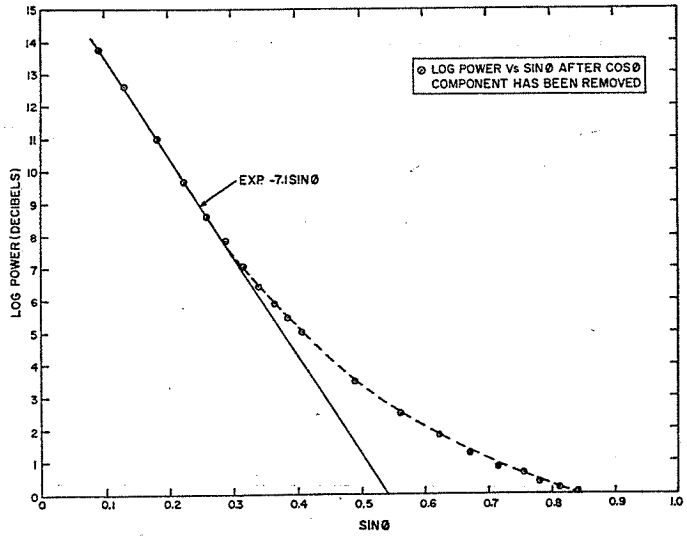


Fig. 16. The variation of the echo intensity at 3.6 cm as a function of sin $\phi$ when the component that obeys the cos $\phi$ law (Figure 15) has been removed.

imply to the improved resolution afforded by ing shorter pulses and conclude, in contrast to ughes [1961], that the law $\bar{P}(\phi) \propto \exp(-A$ $\phi)$ has no general validity.

Measurements made with 30-$\mu$sec pulses can used to compare the scattering behavior at 3- and 68-cm wavelengths. For $\phi \leq 12°$ we

$(\phi) \propto \exp(-7.1\sin\phi)$ at 3.6 cm (13)

$(\phi) \propto \exp(-12.5\sin\phi)$ at 68 cm (10)

measurements made at 68 cm with 12-$\mu$sec ses have a resolution comparable with those de by Hughes at 10 cm, and a proper com- son of the behavior at these two wavelengths the region $3° < \phi < 9°$ is contained in

$(\phi) \propto \exp(-10.2\phi)$ at 10 cm (3)

$(\phi) \propto \exp(-15.3\sin\phi)$ at 68 cm (11)

## Total Reflected Power and Dielectric Constant of the Surface

data presented in Figure 6 have been alized at the origin. The total reflected can be obtained by integrating the area the curve for $\bar{P}(t)$. In this way the radar ection of the moon can be determined, given a knowledge of the equipment parameters (Tables 1 and 2). When expressed as a percentage of the physical cross section presented by the moon's disk ($\pi a^2$) the value obtained at 3.6 cm is $2 \pm 1$ per cent and at 68 cm is $7 \pm 1$ per cent. The 68-cm value is close to that observed by *Fricker et al.* [1960]. The low value obtained at 3.6 cm is in conflict with a value of $7 \pm 2\frac{1}{2}$ per cent obtained at the same wave-

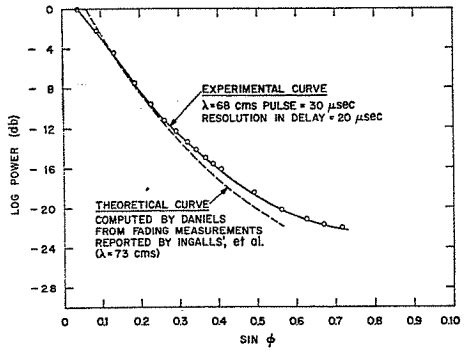


Fig. 17. The variation of the echo intensity at 68 cm shown in Figure 6 with sin $\phi$. A component that appears to obey a $P(\phi) \propto \cos^{3/2}\phi$ has been removed. The results of theoretical calculations by *Daniels* [1961] are shown for comparison.

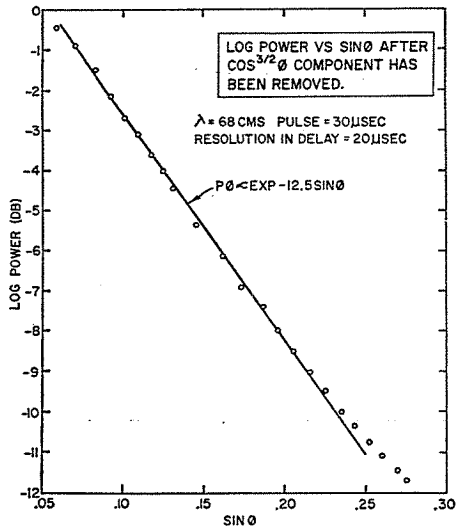


Fig. 18. The variation of the echo intensity with sin $\phi$ at 68 cm shown in Figure 17 for values of sin $\phi < 0.2$.

length by *Morrow et al.* [1962] and may represent an overestimate of the equipment sensitivity by the order of 5 db. The values for the scattering cross section of the moon obtained by various workers using CW or long-pulse transmissions are listed in Table 4 and plotted in Figure 22. The points shown dotted were obtained by *Kobrin* [1959] using a low-power CW bistatic radar. The value Kobrin reported for 3-cm wavelength is in error, because he scaled up the observed cross section by a factor of $(8/5)^2$ to allow for the fact that his beamwidth was comparable in angular diameter with the moon. Such a factor would apply only if the moon were a uniformly bright reflector, and, as little power is reflected from the limbs at this wavelength, Kobrin's (3-cm) value has here been corrected.

The large scatter of values at centimeter wavelengths probably reflects the greater experimental difficulties encountered there by most workers. It seems highly likely that there will be a wavelength dependence in the scattering cross section in view of the fact that the longer wavelengths penetrate more deeply into the surface layer before being reflected. However, the large scatter of the points shown in Figure 22 makes it unwise to infer such a dependence from the present results, and it is important to obtain a value for the cross section at a wavelength in the centimeter region which has an accuracy comparable with that at 1-meter wavelength obtained by *Fricker et al.* [1960].

From a study of the experimental work presented in the preceding sections, we are unable to concur with the conclusion reached by *Senior and Siegel* [1959, 1960] that the principal reflection from the moon's surface is from the first Fresnel zone. The size of the first Fresnel zone for the moon at a meter wavelength is of the order of 1 km across, and it seems unlikely that such a large area would have a height contour that followed the mean surface of the moon to the requisite accuracy, i.e., about ±10 cm. On the contrary, the smooth, monotonic decrease in average echo power from the nearest portion of the moon to the limbs implies a continuous distribution of quasi-specular scatterers which tend to become less favorably orientated at greater delays. We feel, therefore, that the theory presented by Senior and Siegel is based on a

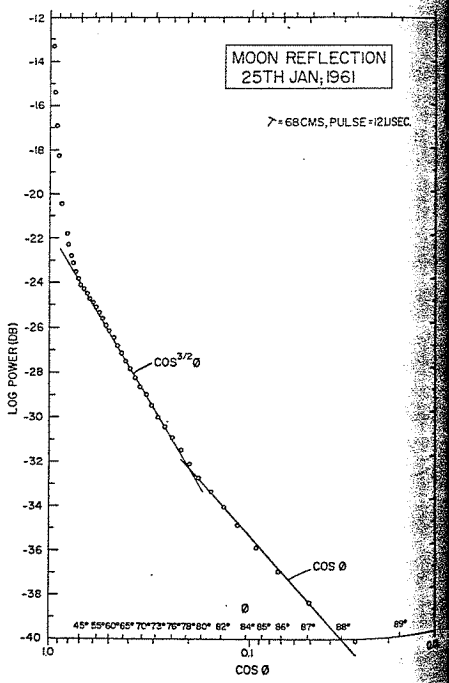


Fig. 19. The average echo power shown in Figure 10 for 12-$\mu$sec observations at 68-cm wavelength is here plotted as a function of log cos $\phi$



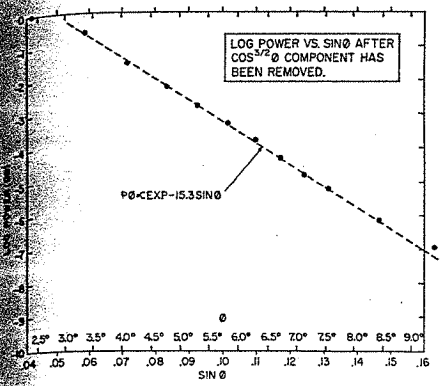


Fig. 20. The average echo power shown in Figure 10 versus sin $\phi$. The components obeying the cos $\phi$ and $\cos^{3/2} \phi$ laws (Figure 19) have been subtracted.

false premise, one that is in direct conflict with the experimental evidence. *Hughes* [1960] and *Hayre* [1961] as well as one of us [*Evans*, 1962*b*] have criticized Senior and Siegel's theory at length, and hence there seems little to be gained by discussing it further. It suffices to say that we do not accept the value $k = 1.1$ for the dielectric constant of the lunar surface obtained by these authors.

The cross section $\sigma$ of a perfectly smooth sphere of radius $a$, made from a material having a reflection coefficient $\rho$ at normal incidence, can be written

$$\sigma = \rho \pi a^2 \tag{14}$$

If the sphere is composed largely of nonconducting materials such as the dry silicate materials that must make up the bulk of the lunar surface, then $\rho$ and $k$ (the dielectric constant) are related in

$$\rho = \left[\frac{\sqrt{k} - 1}{\sqrt{k} + 1}\right]^2 \tag{15}$$

If the surface is irregular (as for the moon) an individual element will scatter back toward the observer in a manner that depends on both its orientation and type of roughness. These effects can be allowed for in the expression for the actual cross section of the entire moon by including in (14) a constant term $g$ which expresses the effective gain brought about by roughening a perfectly smooth sphere

$$\sigma = \rho g \pi a^2 \tag{16}$$

Thus simple, earth-based radar measurements of the total cross section of the moon yield only the product $\rho g$; $g$ must be determined separately in order to determine $\rho$ and thence $k$. The gain $g$ can be calculated if the complete angular scattering law $\bar{P}(i, \phi, \theta)$ is determined. (This law at optical wavelengths is known as the photometric function.) This law specifies the scattering properties of unit area of the surface when illuminated at an angle of incidence $i$ reflecting at an angle $\phi$ (both measured to the normal) and where the angle between the vertical planes containing the incident and reflected rays is $\theta$, as is shown in Figure 23. The gain $g$ is then given by

$$g = \frac{4\pi \int_0^{\pi/2} \bar{P}(\phi) \sin\phi \, d\phi}{\int_0^{\pi/2} \int_0^{\pi/2} \int_0^{2\pi} \bar{P}(i, \phi, \theta) \sin i \sin\phi \, d\theta \, di \, d\phi} \tag{17}$$

which holds where the effects of phase correlation among the surface elements can be neglected. $\bar{P}(\phi)$ is the special case in which $i = \phi$ and

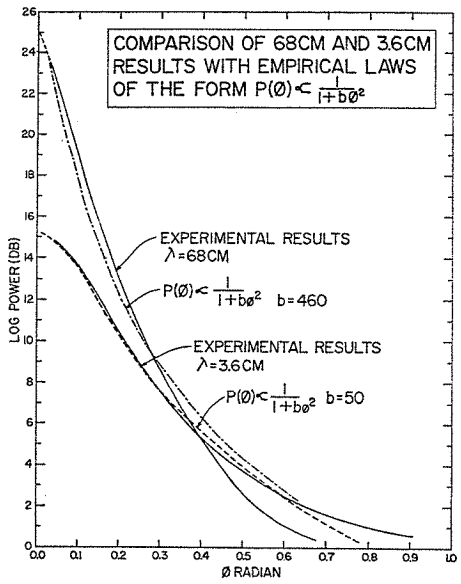


Fig. 21. An empirical law that was found to fit the observations at both 3.6- and 68-cm wavelengths. In both curves the power in the components following cos $\phi$ or $\cos^{3/2} \phi$ (Figures 15 and 19) have been subtracted.

$\theta = 0$. It is clear that the general law $\bar{P}(i, \phi, \theta)$ cannot be determined from earth-based observations alone, as can $\bar{P}(\phi)$. Thus at the present time a rigorous value for $g$ (and thence $k$) is not possible. However, some insight into the most probable values can be obtained from the following arguments. For the 68-cm observations, some 20 per cent of the reflected power appears to obey the law

$$\bar{P}(\phi) \propto \cos^{3/2} \phi \quad (17)$$

whereas approximately 80 per cent of the power is associated with the quasi-specular component which varies as

$$\bar{P}_s(\phi) \propto \frac{1}{1 + 460\phi^2}. \quad (18)$$

The first expression bears some resemblance to Lambert's law

$$\bar{P}(i, \phi, \theta) \propto \cos i \cos \phi \quad (18)$$

which yields a value $g = 8/3$ [*Grieg et al.*, 1948], or another law

$$\bar{P}(i, \phi, \theta) \propto \frac{\cos i}{\cos i + \cos \phi} (1 + \cos^2 \theta) \quad (19)$$

which also approximates to the moon's scattering at optical wavelengths [*Minnaert*, 1961]. When (19) is substituted into (17) and the integration performed numerically, a value $g = 2.68$ is obtained; i.e., the result is indistinguishable from that for Lambert's law. We shall, therefore, suppose that a value $g = 8/3$ is proper for the component expressed by (2).

The principal reflections shown in Figure 6 form a sharp peak near the origin, which is interpreted as being caused by 'mirror-like' reflection from a large number of flat areas many wavelengths across. Echoes from these individual facets interfere with one another, of course, and cause fading in the returned signal as the moon changes its aspect with respect to the radar. By summing the instantaneous responses over a period of time, a statistical picture can be built up of the way in which these facets are distributed in their inclination to the local horizontal, as is discussed in a later section.

*Daniels* [1961] and, later, *Winter* [1962] have shown that, subject to certain approximations probably satisfied here, such a surface exhibits a gain of unity. That such a result should be expected where the mean inclination of the facets is small and their distribution random can also be seen from an argument of plausibility. A smooth sphere much larger than the incident wavelength can easily be shown to scatter isotropically. This property follows immediately from the fact that scattering into each unit of surrounding solid angle can be associated with a corresponding area of the surface that always intercepts the same amount of irradiating flux. Let the surface be broken up into facets as described above, where the mean inclination $\bar{\iota} \ll 1$. The argument can then be made that, for every 'loss' due to unfavorable inclination of an area that originally contributed to scattering into a given solid angle, there will be a statistically equivalent 'gain' from an adjacent region where the same probability of inclination exists. In other words, it is as though pieces of the surface of a smooth sphere had been rearranged over the hemisphery, whereas the direction of the normal to each piece was maintained fixed in space. So long as shadowing is not important, the scattering will remain isotropic and the resulting gain will still be unity. It then follows that only about 8 per cent of the surface is required to be very rough in order to scatter back the fraction of the reflected power (20 per cent) that appears in the diffuse component (equation 2).

If the value for $\rho_s$ obtained by *Fricker et al.* [1960] at a wavelength of 73 cm, i.e., 7.4 per cent, is employed, together with the assumed values for $g$ for the two components stated above, a value for the reflection coefficient (taken to be the same for both components) $\rho = 0.064$ is obtained. This yields a value for the dielectric constant $k = 2.8$ close to that of dry terrestrial sand or pumice, but only about half the value observed for most silicate rocks, which average around $k = 5$. We conclude that the outermost layers of the lunar surface are porous, having a bulk density only about half that of solid rock. If we are prepared to speculate that the diffuse component is caused by boulders or outcroppings composed of solid rock, and that these have a value $k \approx 5$, then the fraction of the surface that must be covered with this rough structure is reduced from 8 to about 5 per cent. This is remarkably close to the value of 4.8 per cent obtained by *Fremlin* [1959] for the fraction of the surface that must be bare rock in order to give a temperature variation of the surface that would fit the infrared observations of *Pettit* [1940].

Passive measurements of very short wavelength ratio emission from the lunar surface by *Salomonovich* [1960] and *Troitski* [1962] seem to give values for $k$ that are lower than the present

TABLE 4

| Author | Wavelength, cm | $\sigma/\pi a^2$ | Approximate Error, db |
|---|---|---|---|
| *Kobrin*, 1959 | 3 | 0.09 | ±1 |
| This paper | 3.6 | 0.02 | ±3 |
| *Morrow et al.*, 1962 | 3.6 | 0.07 | ±1.5 |
| *Kobrin*, 1959 | 10 | 0.27 | ±1 |
| *Hughes*, 1961 | 10 | 0.021 | ±3 |
| *Victor et al.*, 1961 | 12.5 | 0.022 | ±3 |
| Aarons, 1959* | 33 | 0.09 | ±3 |
| *Blevis and Chapman*, 1960 | 61 | 0.05 | ±3 |
| *Fricker et al.*, 1960 | 73 | 0.07 | ±1 |
| Leadabrand, 1959* | 75 | 0.10 | ±3 |
| *Trexler*, 1958 | 100 | 0.07 | ±4 |
| Aarons, 1959* | 149 | 0.07 | ±3 |
| *Trexler*, 1958 | 150 | 0.08 | ±4 |
| Webb, 1959* | 199 | 0.05 | ±3 |
| *Evans*, 1957 | 250 | 0.10 | ±3 |
| *Evans et al.*, 1959 | 300 | 0.10 | ±3 |

* Reported by *Senior and Siegel* [1959, 1960].

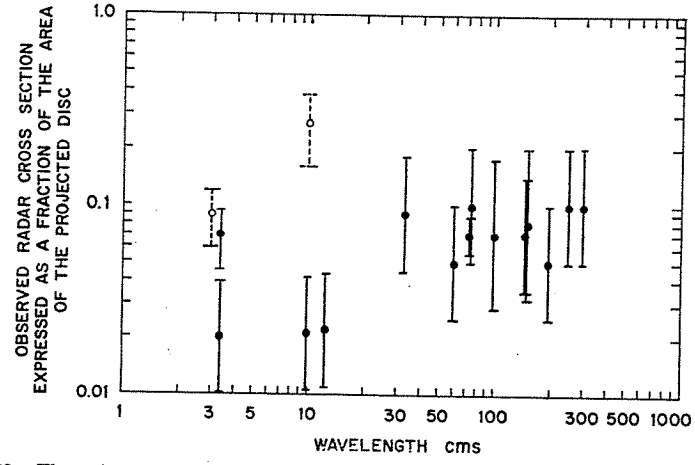


Fig. 22. The values for the radar cross section of the moon expressed as a fraction of the projected area ($\pi a^2$) as a function of wavelength. The points shown dotted were obtained by *Kobrin* [1959] and are discussed in the text.



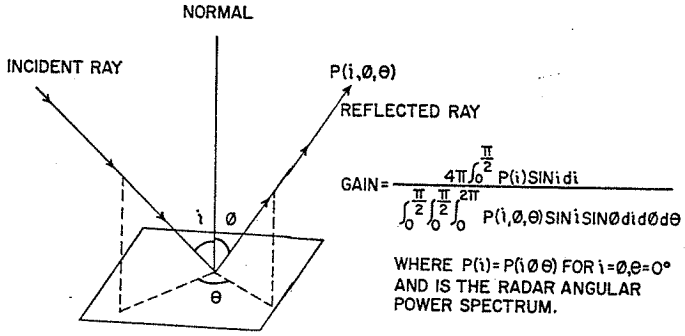


Fig. 23. The geometry required for studying the complete scattering characteristics of an irregular surface in order to obtain a value for the gain of the whole moon over an isotropic scatterer.

results by almost a factor of 2. This discrepancy may be due in part to the fact that neither author allowed fully for surface roughness effects. On the other hand, the microwave measurements may depend on the nature of the material very close to the surface, and the meter-wave radar observations depend on the density farther below the surface. Thus some variation of $k$ with wavelength is perhaps to be expected. As has been noted, the scatter of the values for the cross section at centimeter wavelengths is large, and hence a value for the dielectric constant at these wavelengths derived from the present radar data would be very uncertain.

## 7. Relation between Surface Properties and Scattering Behavior

*Introduction, the diffuse component.* There seem to be several ways in which the surface of the moon might introduce a wavelength dependence into the scattering of electromagnetic radiation. Discounting changes in the reflection coefficient, we find the following. At optical wavelengths the whole surface appears approximately uniformly bright, whereas at 3.6 cm it is only the outer part of the disk ($\phi > 50°$) where this is true. Finally, at 68-cm wavelength only the limb region ($\phi > 80$ per cent) is nearly uniformly bright in appearance. At optical wavelengths where all the power is reflected from rough parts of the surface, there is little tendency for the center of the disk to be any brighter than the rest of the surface. At 3.6 cm, some 70 per cent of the power is returned from the regions that scatter in a quasi-specular manner, whereas at 68 cm 80 per cent is returned from these scatterers. It should, perhaps, be made clear that the separation of the surface elements into those giving rise to quasi-specular scattering and to others giving diffuse scattering is warranted only by the division of the angular power spectrum $\bar{P}(\phi)$ into these two parts (section 5). We do not suppose that the surface has distinctly separate regions that are either smooth or rough, but instead believe that the diffuse component arises from the small-scale elements of a whole distribution of structure sizes. This, then, explains the transition of the scattering behavior from mainly quasi-specular to wholly diffuse as the wavelength is reduced from the order of 1 meter to that of light. As to the size of the irregularities responsible for the diffuse component, we have assumed as a first approximation that they are of the order of the wavelength. The experimental observations of terrestrial surfaces by *Taylor* [1959], however, indicate that for large values of the angle $\phi$ diffuse scattering can occur where the rms size of the irregularities is substantially smaller than the wavelength.

A quantitative theory that takes as its starting point a statistical description of the surface and proceeds to predict the scattering behavior at all wavelengths is lacking at present, although work is being conducted on the problem [*Daniels*, 1963]. Some early attempts to account for the scattering behavior of the moon's surface may be found in *Hargreaves* [1959], *Brown* [1960], *Hagfors* [1961], and *Daniels* [1961], and a brief review of the work reported in these references can be found in *Evans and Pettengill* [1962]. In addition to the above papers dealing solely with scattering from the moon, there are related papers dealing with scattering from the sea [*Daniels*, 1954] or from the ionosphere [*Briggs et al.*, 1950; *Hewish*, 1951; *Bramley*, 1954] that are relevant. The most recently published investigations seem to be those of *Hayre and Moore* [1961] and *Winter* [1962].

It would be out of place here to attempt a detailed review of this theoretical work, and what follows will provide only a brief account. There appear to be no attempts in the literature to account for the diffuse component of the reflected signals. This arises as a consequence of the fact that most authors employ the Kirchoff-Huygens' principle to compute the perturbed electromagnetic field after reflection. Huygens' principle cannot be applied to structure sizes of the order of the wavelength or smaller. Presumably the polarization measurements, when suitably interpreted, can add to our understanding of this fine-scale roughness, but here again suitable theoretical work seems to be lacking.

*Quasi-specular component.* The smoother parts of the surface that are responsible for reflecting the bulk of the energy at radar wavelengths appear more tractable from a theoretical standpoint. Most authors commence with some relatively simple statistical description of the surface from which the scattering properties can be deduced. *Brown* [1960] assumes that the surface can be considered to contain small regions that individually are sufficiently flat to reflect specularly, and that the probability of finding one having a dimension $l$ times $s$ would be

$$\text{probability} = (ue^{-ul}\,dl)(ue^{-us}\,ds) \qquad (20)$$

where $u$ is a roughness coefficient that completely specifies the surface. Predicting the angular power law then becomes a problem of determining the number of specular regions and their average size at different delay intervals. Other authors have attempted to specify the way in which the true height of the surface varies from the mean, and then to describe the horizontal scale of the surface by means of an autocorrelation function. *Hargreaves* [1959], *Hagfors* [1961], *Daniels* [1961], and *Winter* [1962] have all assumed that the distribution of surface heights fits a Gaussian law exp $(-h^2/2\bar{h}^2)$ where $\bar{h}$ is the rms height deviation from the mean. *Hughes* [1962] has criticized *Daniels* [1961] for making this assumption on the grounds that Daniels' theory then leads one to conclude that the scattering should show a wavelength dependence contrary to Hughes' belief [*Hughes*, 1961]. The assumption of a normal distribution of surface heights is not absolutely necessary for the theory, but enormously simplifies the mathematics. It seems clear from the work of *Daniels* [1962] that the exploring wave acts as a linear filter that is insensitive to the form of structure of sizes either very many times the wavelength or smaller than about $\lambda/4$. Thus the height distribution can be allowed to assume almost any form, but radio-echo measurements at a single wavelength can yield information only about a limited range of structure sizes. In consequence, the height distribution would take on the appearance of a Gaussian function in much the same way that wide-band noise passed through a linear electrical filter tends toward a normal distribution of amplitudes (central limit theorem). It seems, therefore, that the assumption of a Gaussian distribution of heights can be retained if the function $\rho(\epsilon)$ that describes the lateral correlation of surface heights is allowed to change with wavelength.

*Bramley* [1954] and others have shown that after reflection at an irregular surface of homogeneous composition the intensity of the field can be regarded as unchanged (close to the surface) and that only phase perturbations are introduced into the wave. If these have a spatial scale described by an autocorrelation function $\rho_E(\epsilon)$, the relationship between $\rho_E(\epsilon)$ and the function that describes the actual surface $\rho(\epsilon)$ is given by

$$\rho_E(\epsilon) = \exp\{-\alpha[1 - \rho(\epsilon)]\} \qquad (21)$$

where $\alpha = 4\pi\bar{h}^2/\lambda^2$ is the rms phase perturbation. The expression given in (21) can be used to obtain $\rho_E(\epsilon)$ if $\rho(\epsilon)$ is known; the angular power law can then be obtained from an equation developed by *Feinstein* [1954]

$$P(\phi) = 2\pi\cos^2\phi\int_0^\infty \rho_E(\epsilon)\epsilon J_0(4\pi\epsilon\phi)\,d\epsilon \qquad (22)$$

The form of the spatial autocorrelation function $\rho(\epsilon)$ assumed by both *Hargreaves* [1959] and *Hagfors* [1961] was Gaussian, namely

$$\rho(\epsilon) = \exp(-\epsilon^2/2\epsilon_0^2) \qquad (23)$$

which in turn leads to an angular power spectrum $P(\phi)$ given by

$$P(\phi) = \exp(-\phi^2/2\phi_0^2) \qquad (24)$$

where $\phi_0 = \bar{h}/\epsilon_0$. The value of $\phi_0$ therefore depends on the ratio of the rms height fluctuation $\bar{h}$ to the horizontal scale distance $\epsilon_0$ and is representative of the average surface gradient.

*Winter* [1962] has examined the case where $\rho(\epsilon)$ is of the form $\rho(\epsilon) = 1 - \epsilon^2/\epsilon_0^2 + \cdots$ for small $\epsilon/\epsilon_0$, and found fair agreement with the results published by *Pettengill and Henry* [1962a].

*Hayre and Moore* [1961] and *Hughes* [1961] have investigated the case in which the spatial autocorrelation function $\rho(\epsilon)$ takes the form of an exponential function

$$\rho(\epsilon) = \exp(-\epsilon/\epsilon') \qquad (25)$$

where $\epsilon'$ is a constant that depends on the scale of the surface. *Hayre and Moore* [1961] arrive at an infinite series for the angular power spectrum, which *Hayre* [1961] claims reduces to *Hughes'* [1960] result

$$P(\phi) \propto \exp(-10.2\phi) \qquad (3)$$

for ratios of $\bar{h}/\lambda = 0.1$ and $\lambda/\epsilon' = 1.0$. It seems probable that these ratios are not unique. *Daniels* [1961] has made use of the fact that for the moon $\bar{h}^2$ (and therefore $\alpha$) is very large, since the optical data published by *Hayn* [1914] yield a value $\bar{h}^2 = 1.85 \times 10^6$ meters$^2$. It follows that $\rho_E(\epsilon)$ in (21) becomes small only for small values

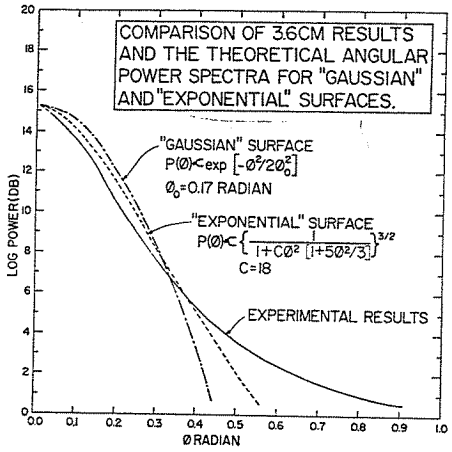


Fig. 24. The values obtained for the echo intensity at 3.6 cm (after the cos $\phi$ component shown in Figure 15 is removed) compared with the best fitting curves for the theoretical laws predicted for a surface having a lateral correlation of surface heights that is Gaussian or exponential.

of $\epsilon$, and hence (25) can be replaced by the first two terms of its expansion without introducing serious error

$$\rho(\epsilon) = 1 - \epsilon/\epsilon' \tag{26}$$

The expression given in (21) can now be used to obtain

$$\rho_E(\epsilon) = \exp\{-\alpha(\epsilon/\epsilon')\} \tag{27}$$

in which $\alpha = (4\pi\bar{h}^2/\lambda^2)$ is to be derived from the optical data. Daniels arrived at a value for $\epsilon'$ from the autocorrelation measurements of the echo amplitude obtained by Ingalls et al. (privately communicated). These autocorrelation measurements are directly related to $\rho_E(\epsilon)$ [*Daniels*, 1961]. Then using a digital computer to solve (22), Daniels obtained the angular power spectrum shown in Figure 17, which provides a fairly good fit to the measured data.

Recently *Hughes* [1962] has published an expression in closed form which represents an approximate solution to (22) when an exponential autocorrelation function $\rho(\epsilon)$ is employed. This law is

$$P(\phi) \propto \left\{\frac{\cos^4\phi}{\cos^4\phi + a\sin^2\phi}\right\}^{3/2} \tag{28}$$

where $a = [\epsilon'\lambda/4\pi\bar{h}^2]^2$, which for small angles can be reduced to

$$P(\phi) \propto \left\{\frac{1}{1 + a\phi^2[1 + (5/3)\phi^2]}\right\}^{3/2} \tag{29}$$

It will be seen that (29) bears a resemblance to the empirical law stated in (12). In Figures 24 and 25 the 'quasi-specular' component observed at 3.6 and 68 cm has been compared with the theoretical laws for the Gaussian (equation 24) and exponential (equation 29) surface autocorrelation functions. The best fitting Gaussian curves have values of $\phi_0$ that differ by a factor of 2. However, the actual values observed are probably not a good measure of the 'average' surface gradients in view of the poor correspondence between the Gaussian law and the experimental results. The exponential model provides a better fit to the data in both cases. The values of the constant $a$ do not vary with wavelength as $\lambda^2$ as might be expected from (28). This can be attributed to the effect mentioned

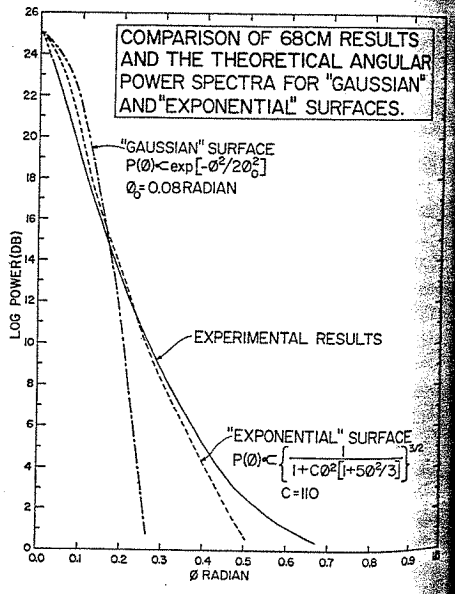


Fig. 25. The values obtained for the echo intensity at 68 cm using 12-$\mu$sec pulses (after the cos $\phi$ and cos$^{3/2}$ $\phi$ components shown in Figure 19 have been removed) compared with the theoretical laws for the angular dependence of the reflected power.



previously; namely, that at a given wavelength $\lambda$ the observations are sensitive to structure with dimensions between $\lambda/4$ and, say, 10–20$\lambda$. Thus at a given wavelength we examine only structure within a given range and therefore only part of the lateral correlation function $\rho(\epsilon)$. Apparently at both 3.6- and 68-cm wavelengths the part of $\rho(\epsilon)$ that can be distinguished is approximately exponential, but one function alone does not describe the behavior at the two wavelengths. If we somewhat arbitrarily equate $\epsilon' = \lambda$ as *Hayre* [1961] has done, then we can obtain values for the ratio $\bar{h}/\epsilon'$ from the values of $a$ in (28) that best match the experimental data. These ratios might be taken as approximate values for the mean gradient of points a wavelength apart. We expect that for a surface such as the moon's, where there is apparently an increasing amount of structure with diminishing size, the average gradient determined in this way would increase as the probing wavelength is reduced. The actual values obtained are $\bar{h}/\epsilon' = 1/11.1$ at $\lambda = 68$ cm and $\bar{h}/\epsilon' = 1/7.4$ at 3.6 cm. A thoroughly rigorous method for deriving the rms surface gradient has been developed by *Daniels* [1963].

## 8. Conclusion

A clear wavelength dependence for the scattering of radio waves by the moon has been established. The meter-wave observations can be explained by a lunar surface 8 per cent of which has structural elements the order of a wavelength in size, whereas the larger structure has a lateral correlation of heights that is best described by an exponential. The mean slope of these larger surface elements appears to be about 1 in 11 (when sampled over intervals of one wavelength). The 7.84-meter observations indicate that at least the smoother parts of the surface scatter as at 68 cm. The dielectric constant deduced from the 68-cm results is $k = 2.8$.

The 3.6-cm observations indicate that 14 per cent of the surface is rough to the order of the wavelength. An exponential autocorrelation function provides a better description of the surface than a Gaussian, though the agreement is not as close as that observed at 68-cm wavelength. It seems plausible that the autocorrelation function that best describes the surface will vary with wavelength, in view of the fact that structure which is substantially smaller than the wavelength has little influence on the scattering behavior. At 3.6 cm the mean gradient over intervals of one wavelength is of the order of 1 in 7.

*Acknowledgments.* We are indebted to numerous colleagues for valuable help in making the measurements described in this paper. In particular we wish to thank B. Nichols and his associates for considerable technical help with the 3.6-cm measurements, also R. P. Ingalls and J. C. James who played a similar part in obtaining the 7.84-meter measurements. We are grateful to R. A. Brockelman who was responsible for the data processing required for the 7.84-meter results, and to W. A. Reid who assisted with all the experiments. We wish to thank D. Karp, W. E. Morrow, and J. H. Chisholm for their interest and encouragement and, finally, Dr. F. B. Daniels for many valuable discussions.

Lincoln Laboratory is operated with support from the U. S. Army, Navy, and Air Force.

## References

Abel, W. G., J. H. Chisholm, P. L. Fleck, and J. C. James, Radar reflections from the sun at very high frequencies, *J. Geophys. Res., 66,* 4303–4307, 1961.

Arthur, J. S., J. C. Henry, G. H. Pettengill, and P. B. Sebring, The Millstone radar in satellite and missile tracking, in *Ballistic Missiles and Space Technology,* vol. 3, p. 81, Pergamon Press, Oxford, 1961.

Blevis, B. C., and J. H. Chapman, Characteristics of 488 megacycles per second radio signals reflected from the moon, *J. Res. NBS, 64D,* 331–334, 1960.

Bramley, E. N., The diffraction of waves by an irregular refracting medium, *Proc. Roy. Soc. London, A, 225,* 515–518, 1954.

Briggs, B. H., G. J. Phillips, and D. H. Shinn, The analysis of observations on spaced receivers of the fading of radio signals, *Proc. Phys. Soc. London, B, 63,* 106–121, 1950.

Brown, W. E., A lunar and planetary echo theory, *J. Geophys. Res., 65,* 3087–3095, 1960.

Browne, I. C., J. V. Evans, J. K. Hargreaves, and W. A. S. Murray, Radio echoes from the moon, *Proc. Phys. Soc. London, B, 69,* 901–920, 1956.

Daniels, F. B., A theory of radar reflection from the moon and planets, *J. Geophys. Res., 66,* 1781–1788, 1961.

Daniels, F. B., Author's comments on the preceding discussion, *J. Geophys. Res., 67,* 895, 1962.

Daniels, F. B., Radar determination of the rms slope of the lunar surface, *J. Geophys. Res., 68*(2), January 15, 1963.

Davies, H., The reflection of electromagnetic waves from a rough surface, *J. Elec. Eng., London,* part 4, *101,* 209–215, 1954.

DeWitt, J. M., Jr., and E. K. Stodola, Detection of radio signals reflected from the moon, *Proc. IRE, 37,* 229–242, 1949.

Evans, J. V., The scattering of radio waves by the moon, *Proc. Phys. Soc. London, B, 70,* 1105–1112, 1957.

Evans, J. V., Radio echo observations of the moon at 3.6 cm wavelength, *Lincoln Lab. MIT TR-256,* 1962*a*.

Evans, J. V., Radio echo studies of the moon, in *Physics and Astronomy of the Moon,* edited by Z. Kopal, Academic Press, New York, 1962*b*.

Evans, J. V., Radio echo observations of the moon at 68-cm wavelength, *Lincoln Lab. MIT TR-272,* 1962*c*.

Evans, J. V., S. Evans, and J. H. Thomson, The rapid fading of moon echoes at 100 Mc/s, *Paris Symposium on Radio Astronomy,* edited by R. N. Bracewell, pp. 8–12, Stanford University Press, Stanford, 1959.

Evans, J. V., and G. H. Pettengill, The scattering properties of the lunar surface at radio wavelengths, in *The Solar System,* vol. 4, edited by G. P. Kuiper and B. M. Middlehurst, University of Chicago Press, Chicago, in press, 1962.

Feinstein, J., Some stochastic problems in wave propagation, part 1, *Trans. IRE, AP2,* 23–30, 1954.

Fremlin, J. H., Sub-surface temperatures on the moon, *Nature, 183,* 1317–1318, 1959.

Fricker, S. J., R. P. Ingalls, W. E. Mason, M. L. Stone, and D. W. Swift, Computation and measurement of the fading rate of moon reflected UHF signals, *J. Res. NBS, 64D,* 455–465, 1960.

Grieg, D. D., S. Metzger, and R. Waer, Considerations of moon-relay communication, *Proc. IRE, 36,* 652–663, 1948.

Hagfors, T., Some properties of radio waves reflected from the moon and their relation to the lunar surface, *J. Geophys. Res., 66,* 777–785, 1961.

Hargreaves, J. K., Radar observations of the lunar surface, *Proc. Phys. Soc. London, B, 73,* 536–537, 1959.

Hayn, F., Selenographische Koordinaten IV, *Sachsische Ak. Wiss. Abh. Math. Phys. K1, 33,* 5–112, 1914.

Hayre, H. S., Radar scattering cross section applied to moon return, *Proc. IRE, 49,* 1433, 1961.

Hayre, H. S., and R. K. Moore, Theoretical scattering coefficient for near vertical incidence from contour maps, *J. Res. NBS, 65D,* 427–432, 1961.

Hewish, A., The diffraction of radio waves in passing through a phase changing ionosphere, *Proc. Roy. Soc. London, A. 209,* 81–96, 1951.

Hey, J. S., and V. A. Hughes, Radar observations of the moon at 10 cm wavelength, *Paris Symposium on Radio Astronomy,* edited by R. N. Bracewell, pp. 13–18, Stanford University Press, Stanford, 1959.

Hughes, V. A., Roughness of the moon as a radar reflector, *Nature, 186,* 873–874, 1960.

Hughes, V. A., Radio wave scattering from the lunar surface, *Proc. Phys. Soc., 78,* 988–997, 1961.

Hughes, V. A., Discussion of paper by Daniels 'A theory of radar reflections from the moon and planets,' *J. Geophys. Res., 67,* 892–894, 1962.

Ingalls, R. P., L. E. Bird, and J. W. B. Day, Bandpass measurements of a lunar reflection circuit, *Proc. IRE, 49,* 631, 1961.

Kerr, F. J., and C. A. Shain, Moon echoes and transmission through the ionosphere, *Proc. IRE, 39,* 230–242, 1951.

Kobrin, N. M., Radio echoes from the moon in the X and S band, *Radiotekhn. i Electron.,* 892–894, 1959.

Leadabrand, R. L., R. B. Dyce, A. Fredriksen, R. I. Presnell, and R. C. Barthle, Evidence that the moon is a rough scatterer at radio frequencies, *J. Geophys. Res., 65,* 3071–3078, 1960.

Minnaert, M., Photometry of the moon, *The Solar System,* vol. 3, edited by G. P. Kuiper and B. M. Middlehurst. Univ. of Chicago Press, Chicago, 1961.

Morrow, W. E., Jr., D. Karp, B. Nichols, and R. V. Locke, Jr., Coefficient of reflectivity of lunar surface at X-band frequencies, paper presented at URSI Spring Meeting, Washington, 1962.

Murray, W. A. S., and J. K. Hargreaves, Lunar radar echoes and the Faraday effect in the ionosphere, *Nature, 173,* 944–945, 1954.

Pettengill, G. H., Measurements of lunar reflectivity using the Millstone radar, *Proc. IRE, 48,* 933–934, 1960.

Pettengill, G. H., and J. C. Henry, Radio measurements of the lunar surface, *The Moon, IAU Symposium 14,* edited by Z. Kopal and Z. K. Mikhailov, Academic Press, London, in preparation, 1962*a*.

Pettengill, G. H., and J. C. Henry, Anomalous radar reflectivity of the lunar crater Tycho, *J. Geophys. Res.,* to be published, November 1962*b*.

Pettengill, G. H., and L. G. Kraft, Jr., Earth satellite observations made with the Millstone Hill radar, in *Avionics Research,* p. 125, Pergamon Press, Oxford, 1958.

Pettit, E., Radiation measurements on the eclipsed moon, *Contrib. Mt. Wilson Obs. 627;* and *Ap. J., 91,* 408–420, 1940.

Salomanovich, A. E., Characteristics of the lunar surface layer, *The Moon, IAU Symposium 14,* edited by Z. Kopal and Z. K. Mikhailov, Academic Press, London, in preparation, 1962.

Senior, T. B. A., and K. M. Siegel, Radar reflection characteristics of the moon, in *Paris Symposium on Radio Astronomy,* edited by R. N. Bracewell, pp. 29–46, Stanford University Press, Stanford, 1959.

Senior, T. B. A., and K. M. Siegel, A theory of radar scattering by the moon, *J. Res. NBS, 64D,* 217–228, 1960.

Spetner, L. M., and L. Katz, Two statistical models of radar terrain return, *Trans. IRE PGAP, AP-8,* 242–246. 1960.

Taylor, R. C., Terrain return measurements at $X$, $K_u$, and $K_a$ band, *IRE Convention Record Part 1,* pp. 19–26, 1959.

Trexler, J. H., Lunar radio echoes, *Proc. IRE, 46,* 256–292, 1958.

Troitski, V. S., Some results of the moon exploration by radiophysical methods, paper presented to COSPAR, Washington, 1962.

Van Diggelen, Utrecht Obs., *Recherches. Astron., 14,* part 2, 1960.

Victor, W. K., R. Stevens, and S. W. Golomb, Radar exploration of Venus, *Jet Propulsion Lab. Tech. Rept. 32-132,* 1961.

Winter, D. F., A theory of radar reflections from a rough moon, *J. Res. NBS, 66D,* 215–226, 1962.

Yaplee, B. S., R. H. Bruton, K. J. Craig, and N. G. Roman, Radar echoes from the moon at a wavelength of 10 cm, *Proc. IRE, 46,* 293–297, 1958.

Yaplee, B. S., N. G. Roman, K. J. Craig, and T. F. Scanlon, A lunar radar study at 10-cm wavelength, *Paris Symposium on Radio Astronomy,* edited by R. N. Bracewell, p. 19, Stanford University Press, Stanford, 1959.

(Manuscript received September 4, 1962; revised October 26, 1962.)